

## Gene Flow and Isolation in the Arid Nearctic Revealed by Genomic Analyses of Desert Spiny Lizards

CARLOS J. PAVÓN-VÁZQUEZ<sup>1,2, ID</sup>, QAANTAH RANA<sup>1</sup>, KEAKA FARLEIGH<sup>3</sup>, ERIKA CRISPO<sup>4</sup>, MIMI ZENG<sup>1</sup>, JEEVANIE LILIAH<sup>1</sup>, DANIEL MULCAHY<sup>5</sup>, ALFREDO ASCANIO<sup>3, ID</sup>, TEREZA JEZKOVA<sup>3, ID</sup>, ADAM D. LEACHE<sup>6, ID</sup>, TOMAS FLOURI<sup>7</sup>, ZIHENG YANG<sup>7, ID</sup>, AND CHRISTOPHER BLAIR<sup>1,8, \* ID</sup>

<sup>1</sup>Department of Biological Sciences, New York City College of Technology, The City University of New York, 285 Jay Street, Brooklyn, NY 11201, USA

<sup>2</sup>Facultad de Estudios Superiores Iztacala, Universidad Nacional Autónoma de México, Colonia Los Reyes Ixtacala, Tlalnepantla, Estado de México, C.P. 54090, México

<sup>3</sup>Department of Biology, Miami University, Oxford, OH 45056, USA

<sup>4</sup>Department of Biology, Pace University, One Pace Plaza, New York, NY 10038, USA

<sup>5</sup>Collection Future, Museum für Naturkunde, Leibniz-Institute for Evolution and Biodiversity Science, Berlin 10115, Germany

<sup>6</sup>Department of Biology & Burke Museum of Natural History and Culture, University of Washington, Seattle, WA 98195, USA

<sup>7</sup>Department of Genetics, Evolution and Environment, University College London, London WC1E 6BT, UK

<sup>8</sup>Biology PhD Program, CUNY Graduate Center, 365 5th Ave., New York, NY 10016, USA

\*Correspondence to be sent to: Department of Biological Sciences, New York City College of Technology, The City University of New York, 285 Jay Street, Brooklyn, NY 11201, USA; E-mail: [christopher.blair10@citytech.cuny.edu](mailto:christopher.blair10@citytech.cuny.edu).

Received 15 May 2023; reviews returned 18 December 2023; accepted 5 January 2024

Associate Editor: Rayna Bell

**Abstract.**—The opposing forces of gene flow and isolation are two major processes shaping genetic diversity. Understanding how these vary across space and time is necessary to identify the environmental features that promote diversification. The detection of considerable geographic structure in taxa from the arid Nearctic has prompted research into the drivers of isolation in the region. Several geographic features have been proposed as barriers to gene flow, including the Colorado River, Western Continental Divide (WCD), and a hypothetical Mid-Peninsular Seaway in Baja California. However, recent studies suggest that the role of barriers in genetic differentiation may have been overestimated when compared to other mechanisms of divergence. In this study, we infer historical and spatial patterns of connectivity and isolation in Desert Spiny Lizards (*Sceloporus magister*) and Baja Spiny Lizards (*Sceloporus zosteromus*), which together form a species complex composed of parapatric lineages with wide distributions in arid western North America. Our analyses incorporate mitochondrial sequences, genomic-scale data, and past and present climatic data to evaluate the nature and strength of barriers to gene flow in the region. Our approach relies on estimates of migration under the multispecies coalescent to understand the history of lineage divergence in the face of gene flow. Results show that the *S. magister* complex is geographically structured, but we also detect instances of gene flow. The WCD is a strong barrier to gene flow, while the Colorado River is more permeable. Analyses yield conflicting results for the catalyst of differentiation of peninsular lineages in *S. zosteromus*. Our study shows how large-scale genomic data for thoroughly sampled species can shed new light on biogeography. Furthermore, our approach highlights the need for the combined analysis of multiple sources of evidence to adequately characterize the drivers of divergence. [Barrier; Colorado River; Continental Divide; isolation by environment; phylogeography; *Sceloporus magister*; *Sceloporus zosteromus*.]

Geographic and temporal patterns of population connectivity and isolation provide information about the ecological and environmental forces driving divergence (Avise 2000). The spatial separation of populations by a geographic barrier is considered to be the most common way in which reproductive isolation arises (Jordan 1905; Mayr 1963). Disparate neutral and adaptive processes acting on the separate populations will result in genetic differentiation (Orr and Smith 1998). Although geographic barriers are important for speciation, similar patterns of population isolation are possible in the absence of any geographic barrier. For example, isolation by distance (IBD)—a positive relationship between geographic and genetic distance—appears to be pervasive (Sexton et al. 2014). Once controversial, there is mounting evidence for isolation by environment (IBE) (Shafer and Wolf 2013; Manthey and Moyle 2015; Myers et al. 2019b), a positive relationship between genetic

and environmental differentiation that is independent of geographic distance (Wang and Bradburd 2014). This pattern can arise from several biological mechanisms, such as selection against immigrants, reduced hybrid fitness, and biased dispersal (Wang and Bradburd 2014). Recent studies have shown that geographic distance and environmental gradients are common and critical enablers of divergence among numerous taxa (Sexton et al. 2014; Myers et al. 2019b; Fenker et al. 2021; Jaynes et al. 2022).

Arid or semi-arid conditions prevail across a large portion of the western Nearctic (Shreve 1942). This large area is biologically and environmentally heterogeneous, and several distinct regions or deserts are identifiable (Fig. 1a) (Environmental Protection Agency 2018). Researchers have long questioned how the distinctive biotas of these deserts have been shaped by the geological history of these harsh habitats. In the last 2 decades,

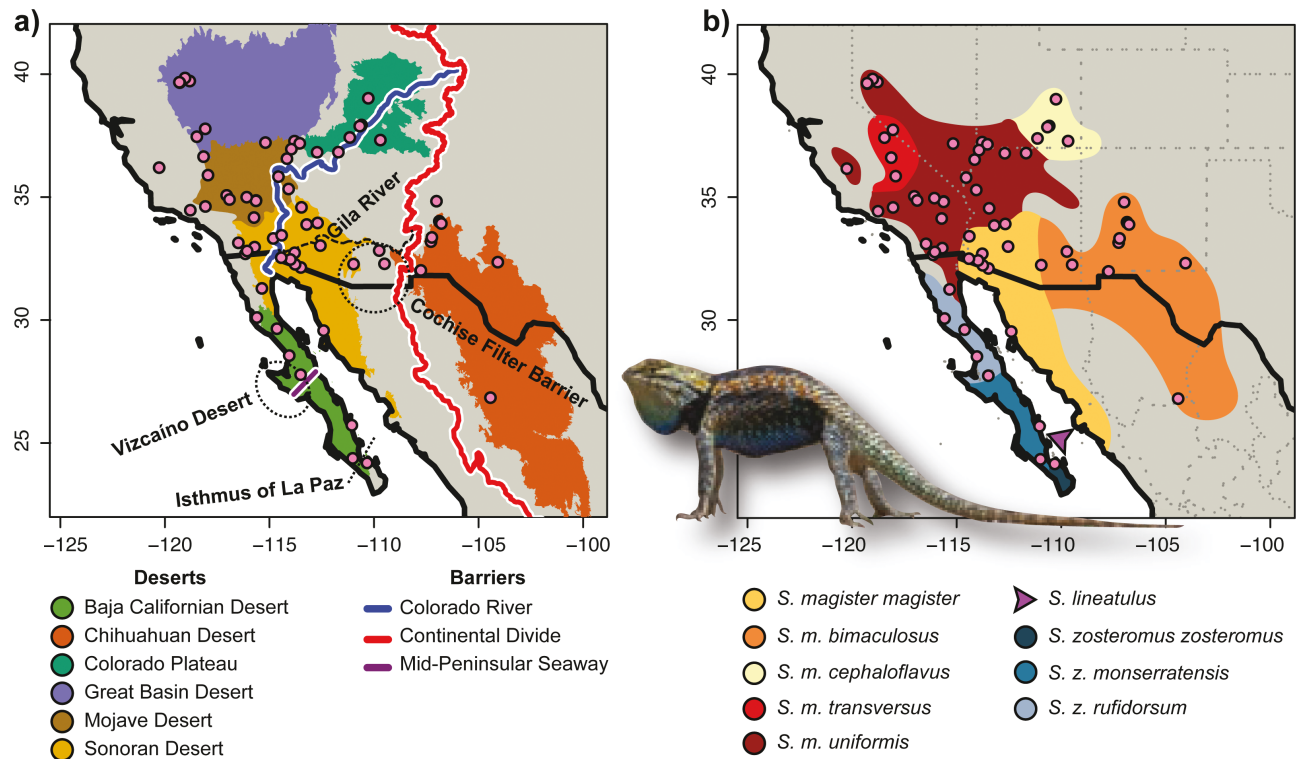


FIGURE 1. Distribution and taxonomy of the *Sceloporus magister* complex across the arid Nearctic. a) Sampling across major deserts of southwestern North America; colored lines represent 3 presumed biogeographic barriers; the dotted circles and lines indicate other regions mentioned in the text, with their names next to them. b) Sampling across the approximate distributions of morphologically defined taxa in the complex (modified from Parker 1982). Photograph by R.C. Clark (Dancing Snake Nature Photography).

molecular data have revealed that many taxa inhabiting these areas are closely related to each other, but geographic structuring and speciation have occurred across this mosaic of deserts (Castoe et al. 2007; Mulcahy 2008; Fehlberg and Ranker 2009; Neiswenter and Riddle 2010; Loera et al. 2012; Chafin et al. 2021; Farleigh et al. 2021). These studies cemented the status of the arid Nearctic as a model system that has exceptionally increased our understanding of the ecological and environmental drivers of diversification.

The enriched knowledge of genetic structure across the arid Nearctic has spawned questions about the factors that promote isolation in the region, facilitating research on the generality and idiosyncrasies of phylogeographic patterns and on the relative roles of barriers, IBD, and IBE. The Chihuahuan and Sonoran deserts are largely separated from each other by high-elevation areas associated with the Western Continental Divide (WCD) (Castoe et al. 2007) (Fig. 1a). These arid regions come into contact in the Cochise Filter Barrier, a low-elevation area along the Arizona–New Mexico border and adjacent portions of northwestern Mexico (Morafka 1977; Castoe et al. 2007). This is an ecotonal region that appears to be an important barrier with variable gene flow across species (Castoe et al. 2007; O’Connell et al. 2017). Another major geographic feature in western North America that appears to be promoting divergence is the Colorado River (Lamb et al.

1992). The bisection of the Baja California Peninsula by a so-called Mid-Peninsular Seaway has been proposed as an explanation for a common geographic pattern of divergence in peninsular taxa (Upton and Murphy 1997; Riddle et al. 2000; Lindell et al. 2006). However, recent comparative studies have questioned the relevance of these presumed barriers. The Cochise Filter Barrier and Colorado River appear to be porous barriers and the degree of differentiation across those features is variable among taxa (Myers et al. 2017, 2019b; Dolby et al. 2019). Some of these differences may be related to organismal traits such as thermal physiology and locomotion (Provost et al. 2021). Additionally, lack of geological evidence and asynchronous divergence in the Baja California Peninsula cast doubt on the seaway hypothesis (Grismar 2002; Leaché et al. 2007). Thus, other factors such as IBD and IBE may be better predictors of genetic differentiation in the arid Nearctic than barriers (Myers et al. 2019b; Dolby et al. 2022). Large datasets and explicit hypothesis testing on suitable systems are necessary to disentangle the effects of barriers, IBD, and IBE.

Desert Spiny Lizards are a group of closely related taxa with a wide distribution in the arid regions of western North America. These lizards constitute the *Sceloporus magister* complex within the *S. magister* group (Schulte II et al. 2006; Leaché and Mulcahy 2007; Leaché et al. 2016). Traditionally, taxa in the complex

were classified as a single species (*S. magister*) with 9 subspecies (Phelan and Brattstrom 1955; Parker 1982): *S. m. magister* from the Sonoran Desert; *S. m. bimaculosus* from the Chihuahuan Desert; *S. m. cephaloflavus* from the Colorado Plateau; *S. m. lineatulus* from Isla Catalina (= Isla Santa Catalina), a deep-water island in the Gulf of California; *S. m. monserratensis* from the Baja California Peninsula between the Vizcaíno Desert and the Isthmus of La Paz (including Isla Monserrate); *S. m. rufidorsum* from the Baja California Peninsula north of the Vizcaíno Desert and south of the mesic forests of the Sierra San Pedro Martir; *S. m. transversus* from the Owens Valley in eastern California and adjacent Nevada; *S. m. uniformis* from the northwestern edge of the Sonoran Desert, the Mojave Desert, and the Great Basin Desert, with a disjunct population in the San Joaquin Valley of California; and *S. m. zosteromus* from Baja California Sur south of the Isthmus of La Paz (Fig. 1b).

Phenotypic variability and the detection of intergradation zones means that the taxonomy of the complex is contentious. Based on morphology, Grismer and McGuire (1996) classified the peninsular subspecies of *S. magister* under a monotypic *S. zosteromus* with the exception of *S. m. lineatulus*, which was regarded as an independent species (*S. lineatulus*). They classified the remaining subspecies under a monotypic *S. magister*. In their checklist of *Sceloporus*, Bell et al. (2003) acknowledged the species status of *S. lineatulus*, *S. magister*, and *S. zosteromus*, but recognized the taxa synonymized by Grismer and McGuire (1996) as subspecies of *S. magister*. Based on ~1700 bp of mitochondrial data from 17 individuals of *S. magister* and 1 *S. zosteromus*, Schulte II et al. (2006) recognized 3 species within *S. magister*: *S. bimaculosus*, *S. magister*, and *S. uniformis*. *Sceloporus m. transversus* was considered a junior synonym of the latter. Finally, Leaché and Mulcahy (2007) used ~1600 bp of mitochondrial data and 4 nuclear loci from ~90 individuals of *S. magister* and 12 *S. zosteromus* to evaluate population structure and gene flow. Their results suggested that *S. magister* should be considered a monotypic but geographically structured species. On the other hand, Leaché and Mulcahy (2007) and Leaché et al. (2016) found *S. lineatulus* (Isla Santa Catalina, BCS, MX) nested among southern populations of *S. zosteromus*, but recommended maintaining both as valid species until further investigation was possible.

In the present study, we infer the geographic and temporal patterns of gene flow and isolation in the *S. magister* complex to obtain a better understanding of the biogeographic processes responsible for shaping lineage divergence throughout the North American deserts. Given the parapatry of lineages and their wide distribution in the deserts of North America, Desert Spiny Lizards constitute an ideal system to evaluate the relevance of geographic and environmental features as obstacles to gene flow and catalysts of isolation. Using many of the same samples used in Leaché and Mulcahy (2007), we generated molecular data consisting of thousands of nuclear loci obtained through high-throughput

sequencing and additional mitochondrial data (up to ~3 kb of concatenated mtDNA). We combined these data with past and present environmental information to identify the drivers of geographic structure. Our broadly applicable workflow tests: (i) whether presumed barriers (the Colorado River, WCD, and Mid-Peninsular Seaway in this case) are effectively acting as barriers to gene flow and to what degree they are responsible for genetic structure; and (ii) whether divergence is driven by physical, spatial (i.e., IBD), or climatic factors (Fig. 2). This approach allowed us to tease apart the effects of biogeographic barriers, geographic distance, and climate in spiny lizards across the arid Nearctic.

## MATERIALS AND METHODS

Here, we outline the methods used for data collection and analysis. We also describe the reasoning behind their implementation and critical methodological decisions. Additional details are presented in the **Supplementary Materials and Methods**.

### Molecular Data

We used a genotyping-by-sequencing (GBS) approach to obtain high-throughput genomic data for 76 individuals of *Sceloporus*: 68 of *S. magister*, 7 of *S. zosteromus*, and 1 of *S. graciosus* to be used as outgroup (Supplementary Table S1). We included samples from the ranges of all morphologically defined taxa in the *S. magister* complex, except for the insular micro-endemic *S. lineatulus* (Fig. 1b). DNA samples were sent to the Biotechnology Center of the University of Wisconsin-Madison for library preparation and sequencing. We processed the raw GBS reads with ipyrad v0.9.87 (Eaton and Overcast 2020). Demultiplexing was followed by adapter removal and filtering of low-quality bases using default values, including no barcode mismatches. Reads were then clustered de novo based on an 85% similarity threshold. Consensus base calling was based on estimates of heterozygosity and rates of sequencing error. This was followed by loci alignment and filtering, aiming to maximize the number of retained loci and informativeness, while minimizing the proportion of missing data (Leaché et al. 2015a; b). We required a locus to be present in at least 50% of samples to be retained in the final assembly. We performed 4 different assemblies using the branching function within ipyrad: all ingroup taxa plus the outgroup (*S. graciosus*), ingroup taxa only, *S. magister* only, and *S. zosteromus* only. Branching was performed after Step 6 in the pipeline to generate different output files. Each of these data sets was used for subsequent analyses (Supplementary Tables S1 and S2).

Additionally, we sequenced the mitochondrial NADH dehydrogenase subunit 1 gene (ND1) and flanking regions. We obtained these sequences from the same specimens that we obtained SNPs from (Supplementary

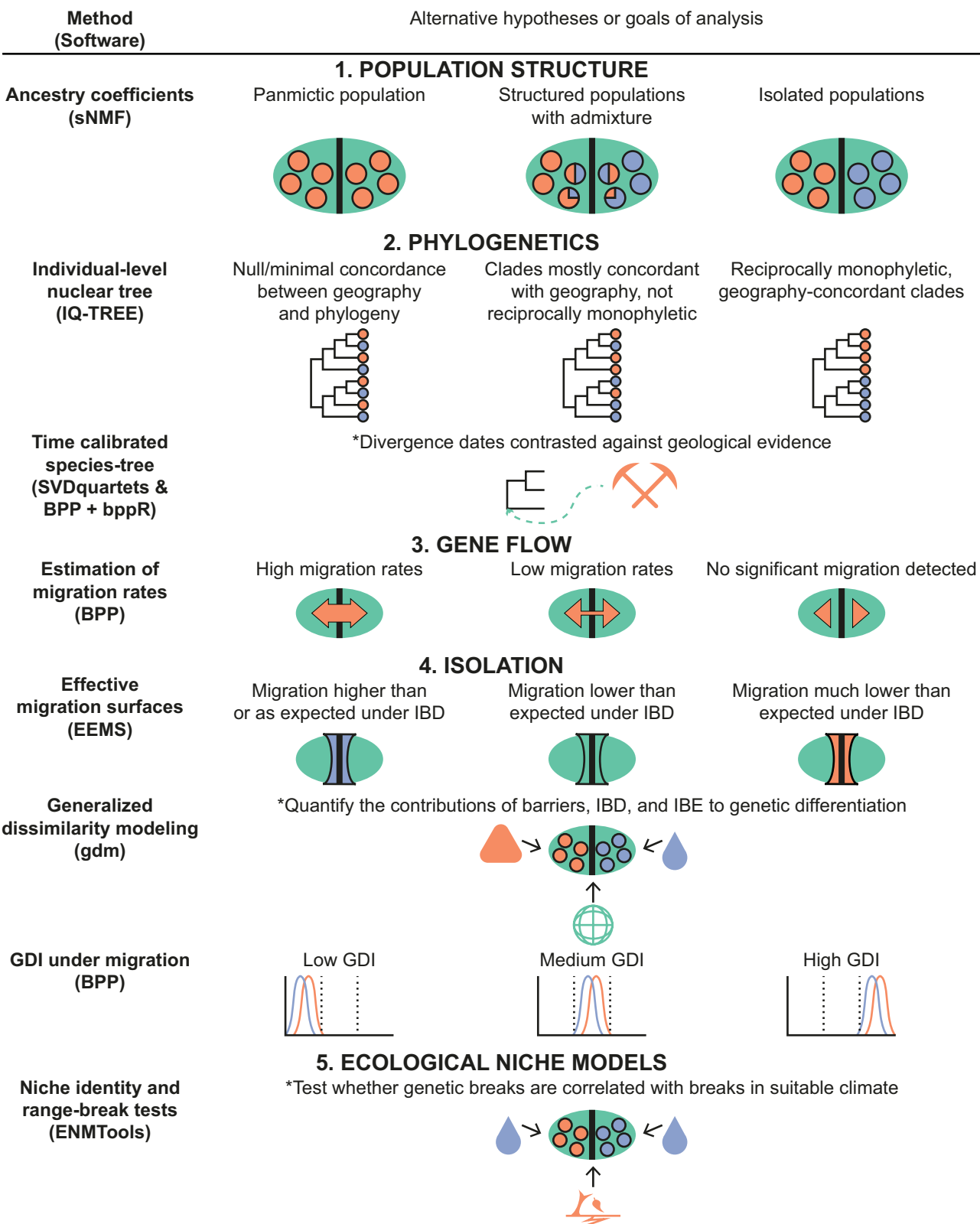


FIGURE 2. Workflow used to test the strength and nature of the drivers of genetic structure. The study area is represented by the oval and a supposed barrier is indicated by the middle line, while the circles represent individuals. For most steps in our approach, 3 possible results related to the strength of the barrier are shown: the left result indicating an nonexistent barrier, the middle a porous barrier, and the right a strong barrier. Asterisks indicate the goals of analyses that aim to test whether the drivers of the structure are physical, spatial (i.e., IBD), or climatic. Abbreviations: GDI = genealogical divergence index, IBD = isolation by distance, and IBE = isolation by environment.

**Table S1**). We then concatenated the newly generated mtDNA data with previous *ND4* ( $n = 63$ ) and *12S* ( $n = 65$ ) sequences from Leaché and Mulcahy (2007). The final alignment included 2923 bp. Newly generated sequences were deposited in GenBank (Supplementary Table S1). *Sceloporus licki* and *S. graciosus* were used as outgroups for the mtDNA analyses.

### Population Structure

We estimated individual ancestry coefficients with sNMF (Frichot et al. 2014) to explore patterns of admixture across presumed barriers. This method bypasses the scalability issues of model-based methods without loss of accuracy by using sparse nonnegative matrix factorization and least squares optimization (Frichot et al. 2014). We conducted independent analyses on each species (*S. magister* and *S. zosteromus*) and on both together. We used the unlinked geno (.u.gen) file output by ipyrad and removed sites with more than 50% missing data. Filtering and sNMF analyses were performed with R (v4.2.1) (R Core Team 2022) and LEA (v3.10.1) (Frichot and François 2015), respectively. We ran analyses under different values of  $K$  (number of populations)—between 1–10 for *S. magister*, and 1–4 for *S. zosteromus*—and selected the value of  $K$  with the lowest cross-entropy. Final analyses for the optimal value of  $K$  were run for 50 repetitions with alpha ( $\alpha$ ) set to 100. We also ran analyses on the dataset containing both species using a fixed value of  $K = 2$  to test for admixture between *S. magister* and *S. zosteromus*. Finally, we also used the same filtered files to perform analysis (PCA) with LEA (v3.10.1) (Frichot and François 2015) using the default settings.

### Phylogenetics

We estimated an individual-level tree based on the GBS data to assess how phylogenetic relationships correlate with geographic origin and taxonomic identity. We used maximum likelihood (ML) as implemented in IQ-TREE (v2.2.0) (Minh et al. 2020). Analyses were based on the full concatenated alignment including invariant sites. The unrooted topologies were subsequently rooted using *S. graciosus*. Support for branches was assessed using both the ultrafast bootstrap (Hoang et al. 2018) and SH-like approximate likelihood ratio tests (Guindon et al. 2010), each with 1000 replicates.

For downstream analyses, we estimated the relationships between the populations identified by sNMF through a species tree approach. First, we estimated relationships with SVDquartets (Chifman and Kubatko 2014) as implemented in PAUP\* (v4.0a) (Swofford 2003). SVDquartets is a coalescent-based method that estimates species (or individual) relationships through quartet analysis. We used the results from the fully sampled sNMF and IQ-TREE analyses to select individuals that had an ancestry coefficient larger than 0.80 for any population (to avoid phylogenetic uncertainty arising from the inclusion of potential hybrids). We also

selected individuals to maximize the geographic representation of each lineage. The data matrix consisted of 22 individuals (including the *S. graciosus* outgroup) and 43,234 SNPs. The u.snps file from ipyrad, which contains a single SNP per locus, was used to minimize the effects of linkage disequilibrium. All quartets were sampled, and support values were obtained from 1000 bootstrap replicates. As a second approach, we performed Bayesian analyses under the multispecies coalescent in BPP (v4.6.2) (Flouri et al. 2018). Analyses were performed on the same individuals that were selected for SVDquartets. Species tree analyses (A01) were run using 1000 loci with analytical phasing (Gronau et al. 2011).

We estimated population sizes and divergence times on the inferred species tree using BPP (A00 analysis). In BPP, population size ( $\theta = 4N\mu$ , where  $N$  is the effective population size and  $\mu$  is the mutation rate per site per generation) is the mean genetic distance within a population. Node ages  $\tau$  are proportional to the expected number of mutations per site. The same loci, individuals, and priors were used for the species tree analysis. We calibrated divergence times ( $\tau$ ) to associate them with known geological events in the arid Nearctic using bppR (Angelis and dos Reis 2015; dos Reis 2022). We assigned a uniform prior (15–21 Ma) for the root age separating the *S. magister* complex from *S. graciosus* based on previous fossil-calibrated analyses (Leaché et al. 2016).

To detect potential mito-nuclear discordance, we estimated the mitochondrial genealogy of the complex. We used both maximum-likelihood (ML) and Bayesian inference to estimate the phylogeny based on the partitioned mitochondrial data. The Bayesian tree was time-calibrated based on a mean rate of 0.00805 substitutions/site/my (standard deviation = 0.001) (Macey et al. 1999; Bryson Jr. et al. 2012).

### Gene Flow

To detect gene flow between the populations identified by sNMF—which are associated with putative barriers (see Results)—we fitted multiple isolation-with-migration (IM) models to the genomic data in BPP. Although many of the algorithms in BPP are based on the MSC model without gene flow, recent additions relax this assumption and allow either episodic introgression (MSci model; Flouri et al. 2020) or continuous migration each generation (IM model; Gronau et al. 2011; Hey et al. 2018). We adopted an analytical approach similar to Ji et al. (2023), where we first fit IM models consisting of a single bidirectional migration event between populations. Migration hypotheses were based on both geography and the results from other analyses. In total, we fit 9 different IM models to the data (Supplementary Table S3). We selected individuals (24 total) throughout the range of each lineage using bpp-tools (<https://github.com/xflouris/bpp-tools>). In contrast to the MSC analyses in BPP, we did not explicitly exclude individuals showing admixture. Each IM analysis was based

on 1000 loci and we specified 2 migration events per analysis (1 bidirectional migration model). Note that the migration rate in BPP is measured in the expected number of migrants per generation.

We used multiple lines of evidence to determine the significance of migration rates inferred by BPP. First, we examined mean migration rates and 95% highest posterior densities (HPDs) to determine if zero was included at the lower bound. Next, we examined the amount of posterior density at zero in Tracer (v1.7.2) (Rambaut et al. 2018). Finally, we calculated Bayes factors (BF) in support of the alternative model of gene flow against the null model of no gene flow using the Savage-Dickey density ratio (Ji et al. 2023). All calculations were done using a custom Python script. We used the cutoff  $BF > 20$  as significant evidence for gene flow; this is similar to the 5% significance level in hypothesis testing. To minimize over-parameterization, we included migration rates only if there was strong evidence for it in the initial runs. Following these initial IM runs, we created a final combined model consisting of all significant migration events. This model was fitted to data of 2500 loci, using 3 independent runs and the same priors as in the previous analyses.

#### Isolation

We estimated effective migration surfaces to infer the geographic location of barriers to gene flow. We used EEMS 0.0.0.900 (Petkova et al. 2016), a Bayesian method that attempts to identify deviations from strict IBD based on a population genetics model. As our measure of genetic differentiation, we calculated average genetic dissimilarity from the SNP matrices used in sNMF (Petkova et al. 2016). We analyzed *S. magister* and *S. zosteromus* independently and divided their range into 500 and 200 demes, respectively. For each dataset, we conducted 3 independent runs which were combined after assessing convergence from the trace plots (Supplementary Fig. S1).

We performed generalized dissimilarity modeling (GDM) to evaluate the importance of geographic distance, biogeographic barriers, and climatic gradients for genetic isolation. GDM is an extension of generalized linear modeling used to analyze data that is best represented as pairwise dissimilarity matrices (Ferrier et al. 2007; Mokany et al. 2022). The method is gaining popularity as a way to identify the drivers of genetic isolation (e.g., Myers et al. 2019b; Jaynes et al. 2022). We analyzed the SNP datasets of *S. magister* and *S. zosteromus* separately. Besides calculating genetic and geographic distances, we obtained the values of 19 climatic variables for each collecting site at a 2.5-min resolution from the WorldClim v2 database (Fick and Hijmans 2017). For *S. magister*, we evaluated the importance of biogeographic barriers in 3 ways: including both the Colorado River and WCD, assigning a value of 1 to individuals west of the Colorado River, 2 to individuals east of the Colorado River and west of the WCD, and 3 to individuals east of the WCD; evaluating the importance

of the Colorado River and coding individuals as occurring west (0) or east of it (1) (a population occurring east of the WCD was not included because it appears to represent the earliest divergence within the species; see 'Results' section); and evaluating the importance of the WCD and coding individuals as occurring west (0) or east of it (1). For *S. zosteromus*, we coded individuals as occurring north (0) or south (1) of the hypothetical Mid-Peninsular Seaway, basing its location on a fine-scale study of genetic structure in *Uta* lizards (Lindell and Murphy 2008). It should be noted that this is not a test for the presence of a seaway *per se*; rather than testing the nature of the barrier, the analysis compares how much genetic variance can be explained by a sharp break versus IBD and IBE. We analyzed climatic data in 2 ways: (i) obtaining climatic distances from the raw values of variables describing annual trends of temperature and precipitation (BIO1 and BIO12), seasonality (BIO4 and BIO15), and extremes (BIO5, BIO6, BIO13, and BIO14); and (ii) calculating distances from the first principal components (PCs) accounting for over 99% of variance, obtained from a PCA of the 19 climatic variables. The second approach was used to minimize the effects of the correlation between climatic variables. Analyses were conducted in the gdm v1.5.0.1 R package (Fitzpatrick et al. 2021). We used the "gdm.partition.deviance" function to calculate the deviance explained by each set of predictors (geographic distances, occurrence on one side or the other for biogeographic barriers, and climatic distances), and the "gdm.varImp" function with default arguments to perform model and variable significance testing and to estimate variable importance through 100 matrix permutations.

We used the genealogical divergence index (GDI) to quantify the degree of genetic divergence between populations (Jackson et al. 2017; Leaché et al. 2019). We implemented a workflow that explicitly integrates gene flow into the calculation of the GDI. Given a locus with 2 sequences  $x_1$  and  $x_2$  sampled from population X and one sequence  $y$  from population Y, the GDI is defined as the probability that  $x_1$  and  $x_2$  coalesce first and before reaching the time ( $\tau$ ) of divergence between X and Y. When there is no gene flow between X and Y, this is also the probability of observing the gene tree topology  $G_X = ((x_1, x_2), y)$ :

$$P_X = P(G_X | \theta_X, \tau) = 1 - \frac{2}{3} e^{-2\tau/\theta_X},$$

where  $\theta_X$  is the population size parameters of X, and where  $e^{-2\tau/\theta_X}$  is the probability that sequences  $x_1$  and  $x_2$  do not coalesce before reaching  $\tau$ . Note that this definition also applies when there is gene flow between X and Y (Kornai et al. 2023). Values close to 1 indicate that X and Y are likely distinct species and values close to 0 indicate that they are likely a single species.

To estimate the GDI under a model that allows for migration between X and Y, we used simulation. We simulated 1 million gene trees for loci with 3 alleles ( $x_1, x_2, y$ ) using BPP estimates of parameters  $\theta_X, \theta_Y, \tau$ ,

and migration rates  $M_{X \rightarrow Y}$  and  $M_{Y \rightarrow X}$  (depending on the assumed migration model). We then calculated the GDI as the proportion of cases in which the gene tree is  $G_x$  and in which the coalescence between  $x_1$  and  $x_2$  is more recent than population divergence at  $\tau$ . As suggested by Jackson et al. (2017), X and Y are considered distinct species if GDI > 0.7 and one single species XY if GDI < 0.2. Intermediate values (0.2 < GDI > 0.7) are considered ambiguous. We conducted this test on the following pairs of lineages (X, Y): MD–SD, SD–MD, CD–(MD + SD), (MD + SD)–CD, NB–SB, and SB–NB (see Results for lineage abbreviations).

### Ecological Niche Models

Finally, we fitted ecological niche models (ENMs) and their derived species distribution models for *S. magister* and *S. zosteromus* to evaluate whether the Colorado River, the WCD, and the putative Mid-Peninsular Seaway represent climatic or geographic barriers for different *Sceloporus* lineages under current conditions. Additionally, we assessed how the geographic ranges of each species have historically responded to contrasting environmental conditions and tested the niche similarity between species and across barriers within species.

Occurrence records for each species were compiled from our sampling database and complemented with VertNet (vertnet.org) records. Bioclimatic variables for present conditions were obtained from WorldClim at 2.5 arcminutes resolution (Fick and Hijmans 2017). Bioclimatic variables for Last Glacial Maximum (LGM; Karger et al. 2023) and Last Interglacial (LIG; Otto-Bliesner et al. 2006) periods were obtained through PaleoClim (Brown et al. 2018). These paleoclimatic datasets are based on the Community Climate System Model. ENMs were fitted to the presence-background data using the MaxEnt algorithm (Phillips et al. 2006) as implemented in the dismo (v1.3.9 R) package (Hijmans et al. 2022). We evaluated the performance of different combinations of MaxEnt feature classes and regularization parameters based on the Corrected Akaike Information Criterion (AICc). Model predictive performance was assessed using partial-ROC Area Under the Curve and omission rate based on testing data.

Selected models were used to predict suitability across the area occupied for both species under: (i) Present conditions, (ii) LGM; and (iii) LIG. For all scenarios, Mobility Oriented Parity (MOP) analysis was performed to determine areas where strict extrapolation occurred, that is, areas with higher prediction uncertainty due to novel environmental conditions not present in the model's calibration regions (Owens et al. 2013). We applied the MOP analysis implemented in the kuenm v1.1.9 R package (Cobos et al. 2019). Additionally, to test the null hypothesis that *S. magister* and *S. zosteromus* have the same niche, niche identity tests (Warren et al. 2008) were performed on model predictions under current climatic conditions, using the ENMTools v1.1.1 R package (Warren et al. 2021). Furthermore, geographic suitability under LGM and

LIG was mapped and qualitatively compared to suitability estimates under the current climate.

To test the hypotheses that climatic barriers may represent sharp environmental gradients splitting the niche of species or lineages under current climatic conditions, sets of niche identity and linear range-break tests were performed across hypothesized barriers (Glor and Warren 2011). Specifically, to test the hypothesis that the Colorado River is a relevant geographic barrier, we divided *S. magister* occurrences at both sides of the river, reconstructed their corresponding niches using MaxEnt default settings, and performed the corresponding tests as implemented in ENMTools (Warren et al. 2021). The same steps were followed for *S. magister* across the WCD, and *S. zosteromus* across the putative Mid-Peninsular Seaway. All permutational tests were done with 99 iterations. Failure to deem any of these barriers as statistically significant indicates that climate conditions across barriers are suitable for the multiple lineages, and thus may serve as evidence of these barriers being geographically but not climatically relevant under present conditions.

## RESULTS

### Data Sets and Population Structure

We generated 4 alternative data sets from the ipyrad assemblies. Characteristics of the 4 assemblies are shown in Supplementary Table S2. All data sets consisted of > 40,000 loci and > 150,000 SNPs. All of the full, concatenated multilocus alignments were > 3 million bp in length.

The fully sampled sNMF analysis included 75 individuals and 40,523 SNPs. For  $K = 2$ , populations corresponded to *S. magister* and *S. zosteromus*. Admixture between them was minimal except in the range of *S. z. monserratensis* in Baja California Sur (Fig. 3a; Supplementary Fig. S2; Supplementary Table S4). The analysis of *S. magister* included 68 individuals and 40,394 SNPs. The optimal  $K$  value was 3 (Supplementary Fig. S3), with populations corresponding roughly to *S. m. bimaculosus* from the Chihuahuan Desert (population CD), *S. m. magister* from the Sonoran Desert (population SD), and the remaining samples distributed predominantly throughout the northwestern portion of the species distribution including the Mojave Desert, Great Basin Desert, and Colorado Plateau (population MD; Fig. 3a; Supplementary Fig. S2). From here on, we use CD, SD, and MD to refer to the clusters identified by sNMF. Noteworthy admixture between the populations occurring west and east of the WCD was limited to a single individual from southeastern Chihuahua, Mexico. The distributions of SD on one side and MD on the other seem to be demarcated loosely by the Colorado River, but there was considerable admixture between SD and MD. The analysis of *S. zosteromus* included 7 individuals and 37,333 SNPs. For the

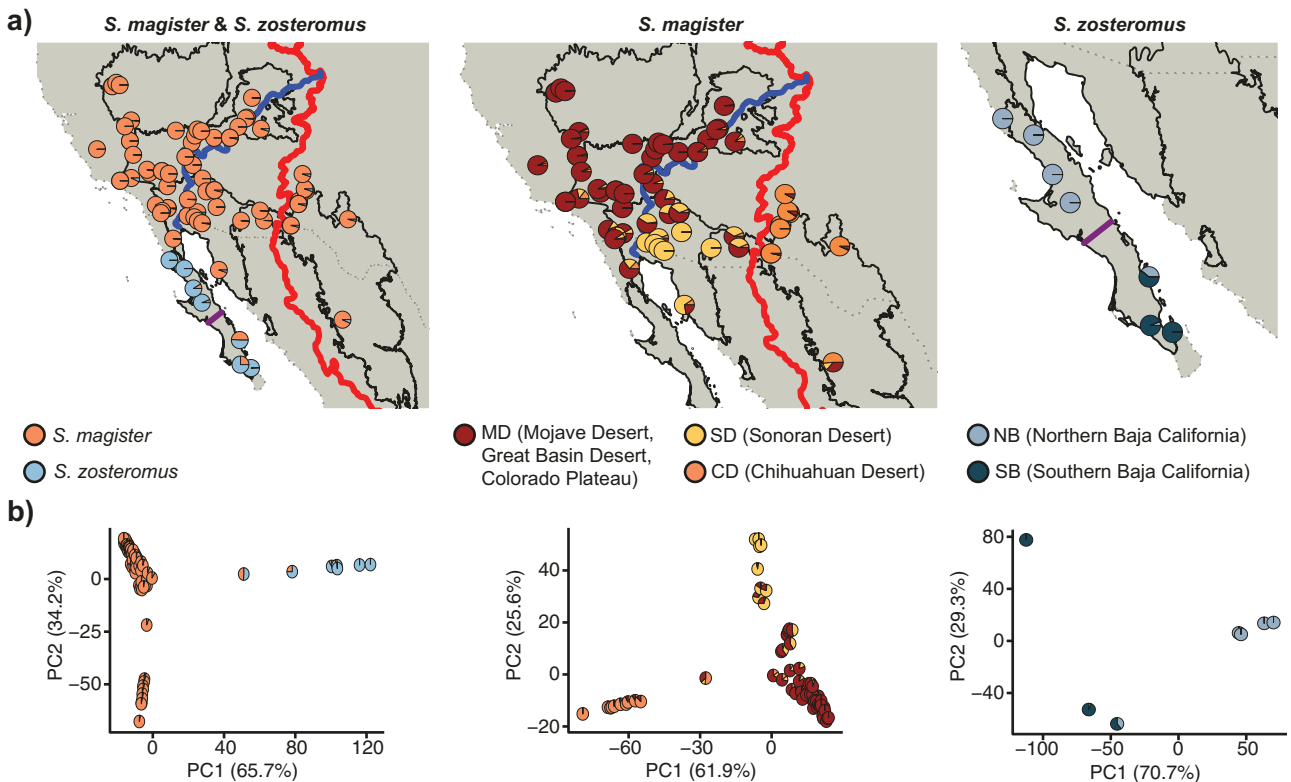


FIGURE 3. Population structure in the *Sceloporus magister* complex. a) Ancestry coefficients inferred by sNMF; each circle corresponds to an individual, solid lines represent the desert borders, dotted lines indicate country limits and other lines represent biogeographic barriers. b) PC analyses; individuals are colored according to the sNMF ancestry coefficients; the percentage of variance explained by each PC is shown in parentheses.

optimal value of  $K$  (2; [Supplementary Fig. S3](#)), populations corresponded to *S. z. rufidorsum* from the Baja California Peninsula, north of the alleged location of the Mid-Peninsular Seaway (population NB/light blue); and *S. z. monserratensis* and *S. z. zosteromus* from south of the Seaway (population SB/dark blue). There was substantial admixture between these populations at one locality ([Fig. 3a](#); [Supplementary Fig. S2](#); [Supplementary Table S4](#)).

In the PCA including both species, PC1 explained 65.7% of the variance separating *S. magister* and *S. zosteromus*, with the admixed individuals from Baja California Sur approaching *S. magister*; PC2 explained 34.2% of the variance and separated CD from other *S. magister* populations, with the specimen from southeastern Chihuahua halfway between the 2 clusters ([Fig. 3b](#)). In the PCA of *S. magister*, PC1 explained 61.9% of the variance and separated CD from other *S. magister* populations, with the Chihuahuan individual showing an intermediate value again; PC2 explained 25.6% of the variance and separated SD from MD ([Fig. 3b](#)). For *S. zosteromus*, PC1 explained 70.7% of the variance and separated NB and SB; PC2 explained 29.3% of the variance and separated an individual from near Loreto (*S. z. monserratensis*) from other individuals in SB ([Fig. 3b](#)).

### Phylogenetics

The ML analysis of the GBS data was based on 76 individuals and 3,171,123 bp. Including the outgroup, 3,019,868 sites were constant, 66,685 sites were singletons, and 84,570 sites were parsimony informative. BIC indicated that a FreeRates model (Yang 1995; Soubrier et al. 2012) fit the data better than the GAMMA model (11,889,138 vs 11,960,418). *Sceloporus magister* and *S. zosteromus* were reciprocally monophyletic with full support. A lineage consisting of samples allied to *S. z. rufidorsum* (NB) was sister to a clade distributed throughout the southern portion of the peninsula (SB). Within *S. magister*, a strongly supported clade corresponding to samples from the Chihuahuan Desert east of the WCD appeared as a sister to all other samples. A strongly supported Sonoran Desert clade (SD) was sister to the remaining individuals. The final major lineage consisted of individuals distributed throughout a broad geographic area encompassing portions of the Mojave Desert, Great Basin Desert, northwestern Sonora Desert, and Colorado Plateau (MD; [Fig. 4a,b](#); [Supplementary Fig. S4](#)). In general, the phylogenetic results were highly congruent to those from sNMF.

The SVDquartets and BPP analyses yielded identical species tree topologies ([Fig. 4c](#)), which were also concordant with the inter-population relationships in

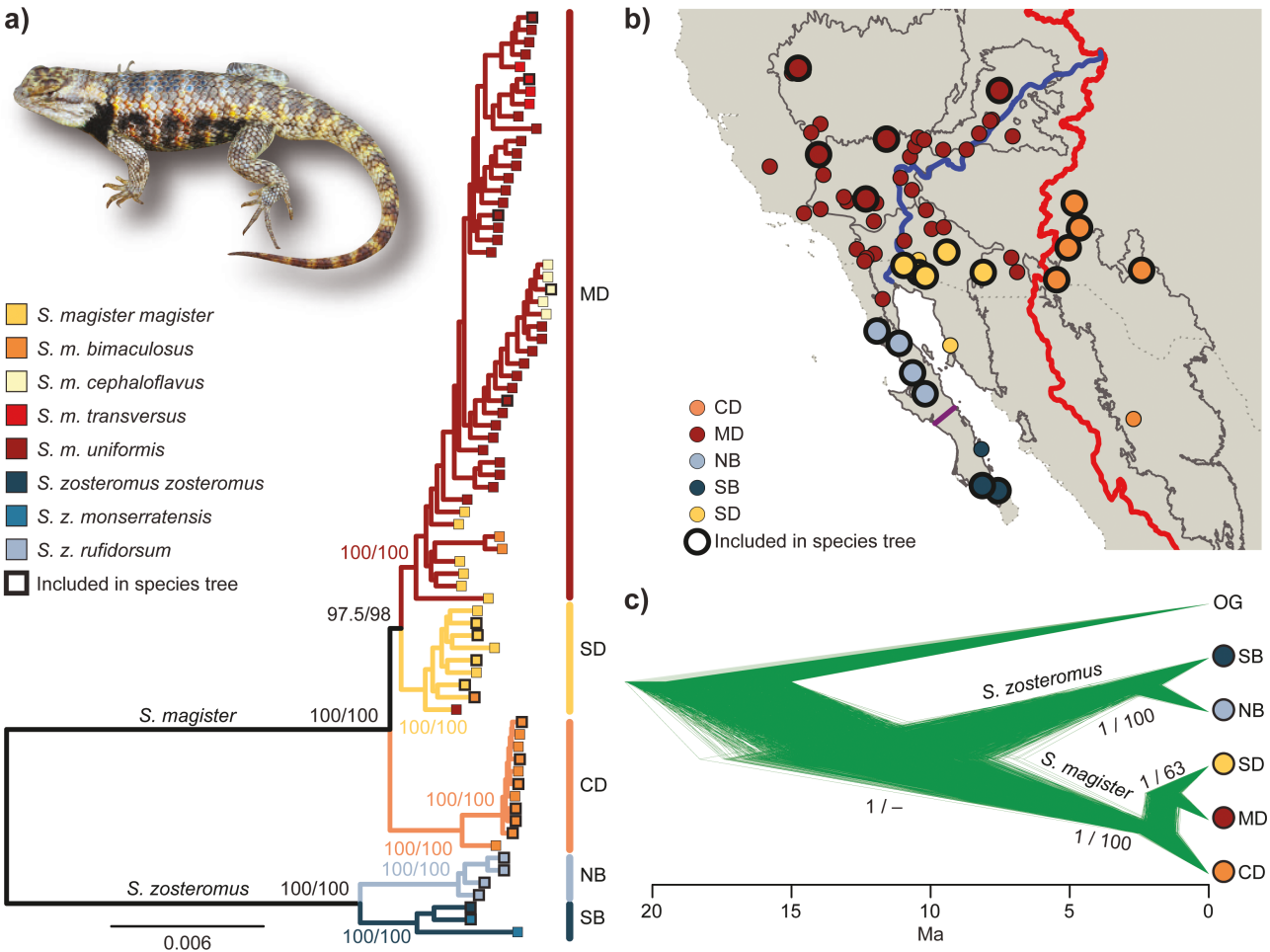


FIGURE 4. Nuclear phylogeny of the *Sceloporus magister* complex. a) ML individual-level tree; numbers on branches represent support values for major lineages (SH-aLRT/ultrafast bootstrap); branch colors and bars right of the tree indicate sample and clade assignments to the populations identified by sNMF (Fig. 3); branch lengths are proportional to substitutions per site; squares next to tips indicate their subspecific identity following Fig. 1b. b) Distribution of the lineages identified in Fig. 4a; map as in Fig. 3a. c) Time-calibrated species tree; divergence times were calculated in BPP; numbers on nodes indicate BPP posterior probabilities and SVDquartets bootstrap values, in that order; each line represents a species tree topology inferred by BPP; individuals included in the species tree are indicated by their bold outlines in the other panels. Photograph by A.G. Clause.

the concatenated ML genealogy. The 3 independent BPP runs converged on the same topology with strong posterior probability (1.0). *Sceloporus magister* and *S. zosteromus* were both reciprocally monophyletic with full support. BPP provided full support for the sister relationship of MD and SD, whereas this node had a bootstrap support of 63. The 2 independent BPP A00 runs converged to similar posterior distributions with virtually all ESS values  $> 200$ . The only parameter with an ESS  $< 200$  was the population size of the ancestor of MD + SD. However, the ESS value was  $> 100$  and qualitative analysis of the marginal density of both runs showed excellent concordance. The size of the CD population was substantially smaller than all remaining populations (Supplementary Table S5). *Sceloporus zosteromus* diverged from *S. magister* during the Miocene approximately 10 Ma (Fig. 4c). The 2 peninsular populations of *S. zosteromus* diverged at the

Pliocene-Pleistocene boundary, whereas all divergence times within *S. magister* fell in the Pleistocene. The estimated substitution rate was 0.000843 substitutions per site per million years (95% HPD interval = 0.000646, 0.0011), similar to other recent genomic studies of lizards (Perry et al. 2018; Finger et al. 2022).

The mitochondrial trees obtained with IQ-TREE and BEAST were similar to each other but differed from the ML tree based on the GBS data (Supplementary Figs. S5 and S6). In the mtDNA gene trees, the MD and SD populations were not monophyletic. Instead, samples from SD were scattered among a handful of MD individuals. A strongly supported CD lineage, east of the WCD, was sister to the remaining samples from MD. This MD lineage was moderately supported. The gene tree divergence times estimated by BEAST were older, on average, than those estimated by BPP for the GBS data.

### Gene Flow

Bayes factor calculation under the IM model in BPP ([Supplementary Table S3](#)) indicated low but significant gene flow within *S. zosteromus* from northern Baja California (NB) to southern Baja California (SB). There was also significant bidirectional gene flow between the SD and MD populations of *S. magister*. No significant migration was detected that involved ancestral populations, and there was no significant gene flow to or from CD. Parameter estimates of the full migration model (with the 3 significant migration events) are shown in [Supplementary Table S6](#). Explicitly accounting for migration had substantial effects on demographic parameters (compare [Supplementary Tables S5 and S6](#)). The final full demographic model is shown in [Fig. 5](#). Migration rates were higher from MD into SD than vice versa. While the rate  $M_{NB \rightarrow SB} = 0.0512$  is lower than the rate between SD and MD (0.149 and 0.403), the former gene flow was over a much longer time period. Note that the impact of gene flow depends on both its rate ( $M = Nm$ ) and its time duration. The CD population had the smallest size of any contemporary or ancestral population. Interestingly, the 2 divergences within the *S. magister* clade were nearly synchronous.

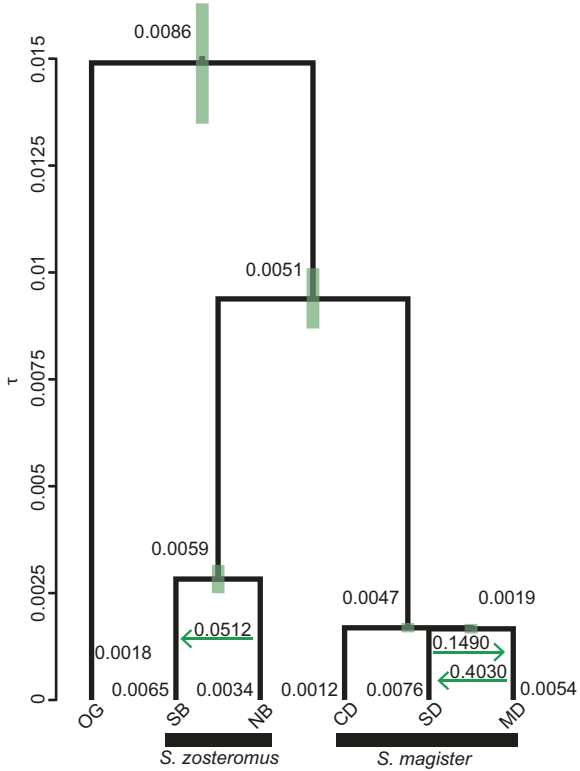


**FIGURE 5.** Full demographic model estimated by isolation-with-migration (IM) analyses in BPP. The y-axis represents divergence times ( $\tau$ ), whereas values at nodes show population sizes ( $\theta$ ). Arrows indicate 3 significant migration events with the mean migration rate above. Node bars represent 95% HPDs for node height. OG = outgroup, other acronyms as in [Fig. 3a](#).

The SB population of *S. zosteromus* was larger than the NB population.

### Isolation

Within the range of *S. magister*, EEMS detected several areas where effective migration was lower than expected under a pure IBD model ([Fig. 6a](#)). These areas overlap with the WCD (including the Cochise Filter Barrier), the mountains surrounding the Colorado Plateau, and the lower Colorado River. Regarding *S. zosteromus*, effective migration rates were low throughout most of the southern half of the peninsula, particularly near the Isthmus of La Paz. ([Fig. 6a](#)). Effective migration around the putative Mid-Peninsular Seaway region was lower than expected under a pure IBD model. Effective diversity for *S. magister* was high throughout the Sonoran Desert and Lower Colorado River Valley ([Fig. 6b](#)), whereas diversity in *S. zosteromus* was concentrated throughout the southern half of the Peninsula of Baja California ([Fig. 6b](#)).

The GDM suggested that biogeographic barriers have the largest impact on genetic differentiation in *S. magister* ([Fig. 7](#)). Across all the analyses, barriers explained the largest proportion of the deviance in genetic distance, both alone and jointly with other predictors. In *S. magister*, the Colorado River had less predictive power than the WCD. Furthermore, climate had strong predictive power in the analyses that focused exclusively on the Colorado River. In the case of *S. zosteromus*, climate explained most of the deviance in genetic distance when its joint effect with other predictors was considered and the climatic variables were analyzed raw. The Mid-Peninsular Seaway had the largest joint effect when the PCs of the climatic variables were used. Regardless of how the climatic data were included, climate had the largest independent predictive power for *S. zosteromus* ([Fig. 7](#)). All the full models were significant and explained between 71.80% and 93.90% of the deviance in genetic distances. Additional details on the models, predictor importance, and predictor significance are presented in [Supplementary Tables S7–S9](#).

The GDI values were above the 0.7 threshold for the bidirectional CD  $\leftrightarrow$  MD + SD comparisons, suggesting that CD is a genetically distinct species from MD and SD according to the GDI criterion ([Table 1](#)). In addition, GDI was 0.793 for the NB/SB comparison, indicating that the population in northern Baja California is distinct from the population in southern Baja California. We note that the GDI for SB versus NB was 0.540 (below the 0.7 threshold). However, the discrepancy can be explained by the larger population size of SB. The GDI values for the MD-SD and SD-MD comparisons were below 0.7, suggesting that these populations do not represent distinct species.

### Ecological Niche Models

Species distribution model predictions for the present, LGM, and LIG are found in [Supplementary Fig. S7](#). Model features are detailed in [Supplementary Table](#)

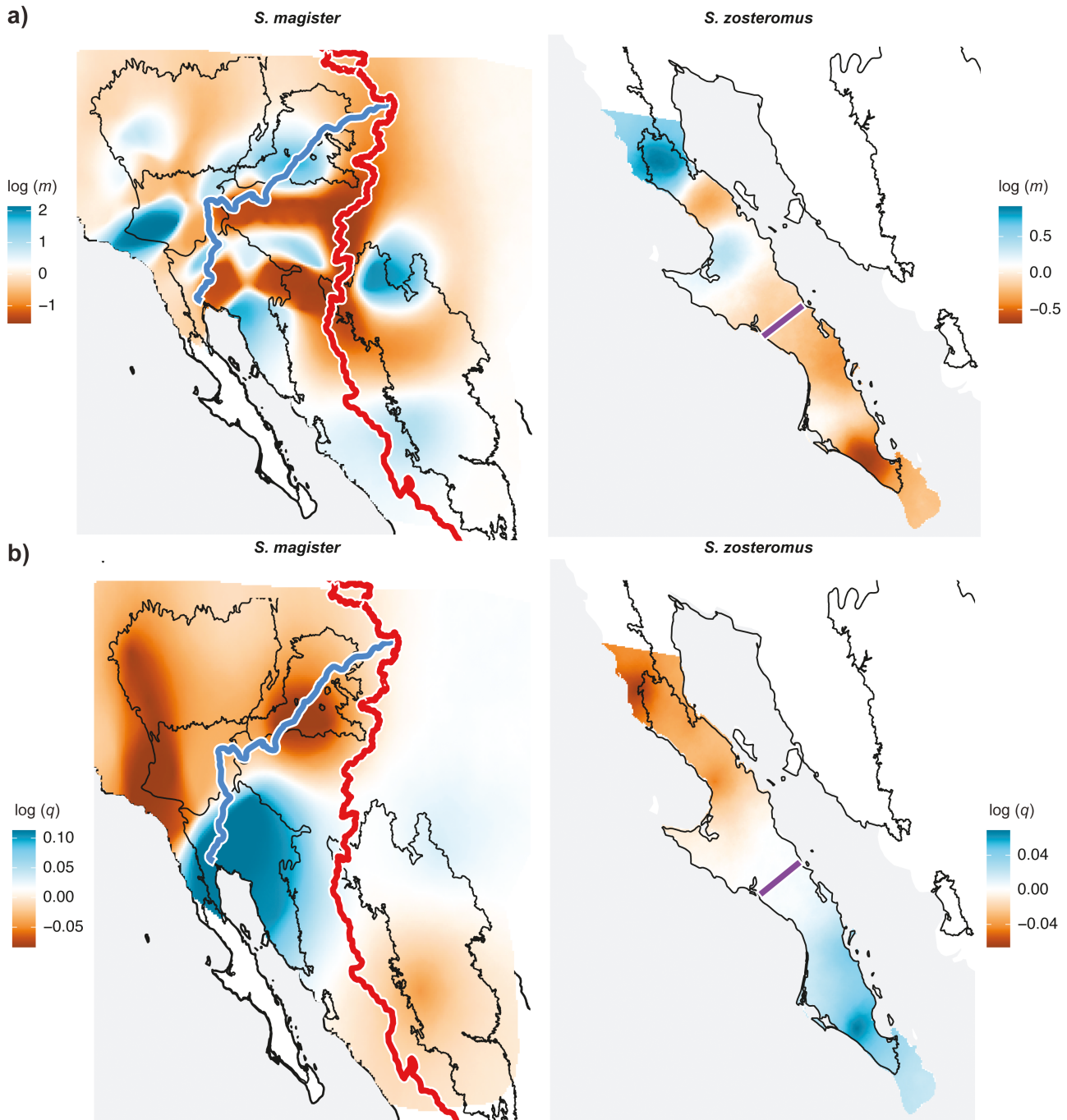


FIGURE 6. Geographic variation in effective migration (a) and effective diversity (b). Maps as in Fig. 3a.

**S10.** MOP showed robust SDM predictions under current and past climate scenarios, with regions of strict extrapolation outside of the areas of interest for each species (Supplementary Fig. S8). Comparisons between both species presented statistically significant differences according to niche identity tests (Table 2).

The climatic variables with the largest contribution to the distribution model of *S. magister* were (in order) annual precipitation, temperature seasonality, mean

temperature of the coldest quarter, and precipitation of the driest month (Supplementary Table S11). The variables with the largest permutation importance were (in order) temperature seasonality, mean temperature of the coldest quarter, and precipitation of the wettest quarter (Supplementary Table S11). The Cochise Filter Barrier was identified as an area of low climatic suitability, especially for the LGM prediction, which more generally showed a contraction of suitable habitat

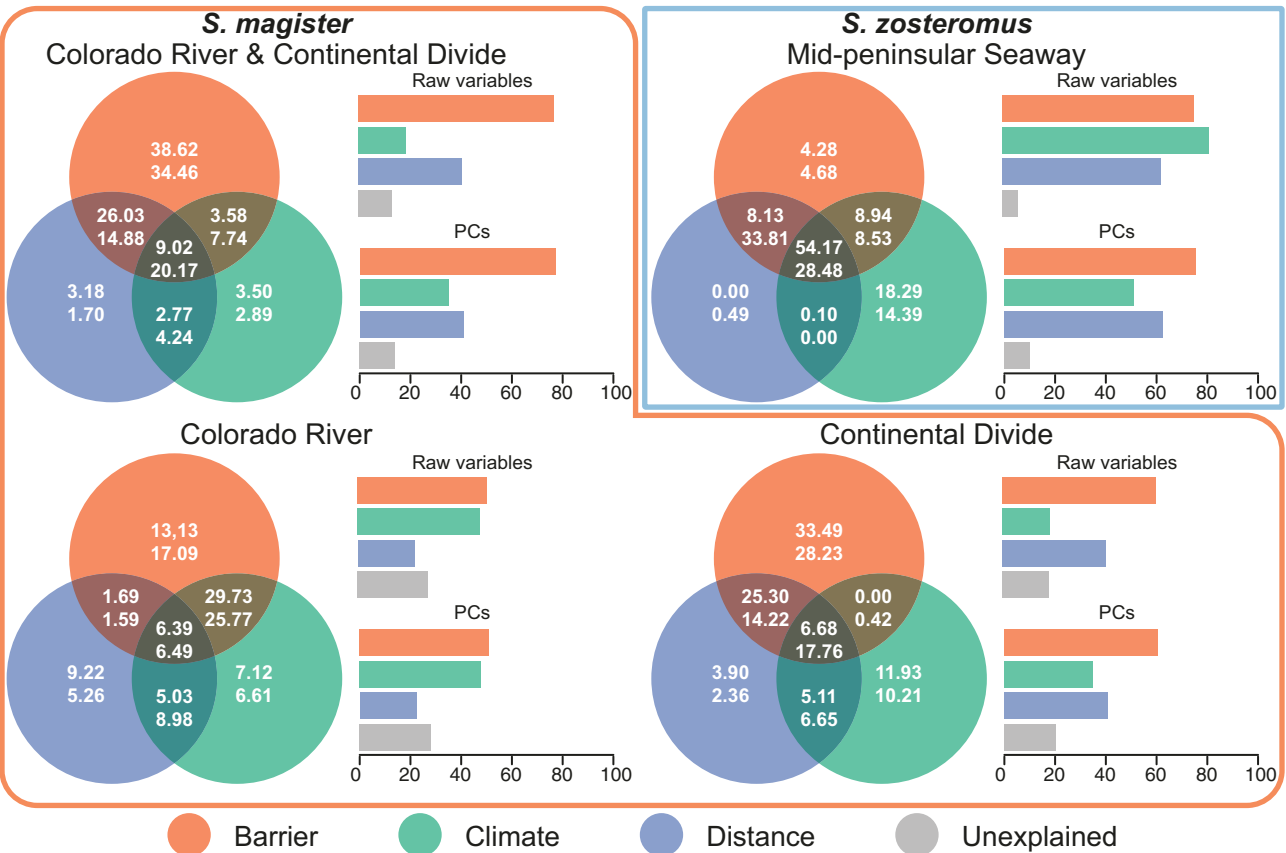


FIGURE 7. Deviance in genetic distances explained by biogeographic barriers, climate, and geographic distances. Values at the center of each circle in the Venn diagrams are the % deviance explained by each set of variables alone, while values at the intersections are the deviance explained by that section of the intersection alone; that is, all values inside a circle need to be added to get the total deviance explained by a given set of variables; values on top were obtained from an analysis where climate was represented by 8 variables describing annual trends, seasonality, and extremes in temperature and precipitation; values on bottom were obtained from an analysis where climate was represented by the PCs of 19 climatic variables. Bar plots indicate the total deviance explained by each set of variables (see text for details).

TABLE 1. GDI for major lineages of the *Sceloporus magister* complex

X-Y	MD-SD	SD-MD	CD-(MD + SD)	(MD + SD)-CD	SB-NB	NB-SB
GDI	0.385	0.271	0.934*	0.813*	0.540	0.793*

Note: The GDI for the X-Y comparison uses 2 sequences from X and 1 sequence from Y and indicates the distinct species status of X relative to Y. Asterisks indicate significant evidence for isolation.

(Supplementary Fig. S7). Furthermore, niche identity showed statistically significant differences between niche models built after splitting occurrences west and east of the WCD. In addition, linear range break tests determined that these differences could be due to steep climatic differences on both sides of the climatic barrier (Table 2).

The lower Colorado River does not appear to be associated with an area of low climatic suitability (Supplementary Fig. S7). ENMs generated by dividing species occurrences north and south of this barrier showed statistically significant differences according to the identity test (Table 2). Despite these differences, a linear range break test confirmed that the Colorado River itself does not present a statistically significant climatic barrier (Table 2), indicating that other non-climatic

factors may be driving the differences in observed suitability across both sides of the barrier. Large portions of the southern United States and northern Mexico were recovered as suitable in the LIG prediction.

For *S. zosteromus*, the climatic variables with the largest contribution were (in order) precipitation of the driest month, temperature seasonality, mean annual precipitation, and precipitation of the coldest quarter (Supplementary Table S11). Precipitation of the driest month and precipitation of the wettest quarter had a larger permutation importance than other variables. The supposed location of the Mid-Peninsular Seaway coincided with an area of relatively low climatic suitability, particularly under current and LIG climatic conditions (Supplementary Fig. S7). Despite this, no relevant differences were found with identity and linear

TABLE 2. Statistical significance of Ecological Niche Model (ENM) comparisons under current climatic conditions and across hypothesized barriers and species

Species	Test	Barrier	Schoener's <i>D</i> ( <i>p</i> )	Hellingers' <i>I</i> ( <i>p</i> )
<i>S. magister</i> – <i>S. zosteromus</i>	Identity	–	0.083 (0.01*)	0.234 (0.01*)
<i>S. magister</i>	Identity	Colorado River	0.094 (0.01*)	0.228 (0.01*)
	Range break	Colorado River	0.094 (0.16)	0.228 (0.2)
	Identity	Continental Divide	0.039 (0.01*)	0.161 (0.01*)
	Range break	Continental Divide	0.039 (0.01*)	0.161 (0.01*)
<i>S. zosteromus</i>	Identity	Mid-Peninsular Seaway	0.977 (1)	0.999 (1)
	Range break	Mid-Peninsular Seaway	0.977 (1)	0.999 (1)

range break tests between ENMs built by splitting occurrences north and south of this barrier (Table 2). Suitable habitat becomes largely restricted to the southern portions of the Baja California Peninsula in the LIG prediction (Supplementary Fig. S7).

## DISCUSSION

Our analyses indicate that the evolutionary history of the *S. magister* complex in western North America has been characterized by instances of isolation and gene flow. Results suggest that biogeographic barriers played an important role in genetic differentiation, but the nature and strength of barriers varied across the group's range. Below we discuss the evolutionary history of this species complex, highlighting how the incorporation of molecular and environmental data is necessary to tease apart the drivers of geographic structure.

### Speciation Between *S. magister* and *S. zosteromus*

The phylogenomic chronogram that we used as a guide to calibrate our GBS trees relies on a deep calibration, far from the *S. magister* complex (Leaché et al. 2016). Still, the estimated ages for the split between *S. magister* and *S. zosteromus* are similar between the tree of Leaché et al. (2016), previously published mitochondrial trees (Leaché and Mulcahy 2007), and our own trees based on the GBS data. They all suggest a Late Miocene divergence which, as previously noted (Schulte II et al. 2006; Leaché and Mulcahy 2007), is consistent with the Middle to Late Miocene origin of the Gulf of California (Ferrari 1995; Lee et al. 1996). Our mitochondrial analyses suggest a slightly earlier divergence, but this could be caused by substitution saturation in our mitochondrial fragments (Zheng et al. 2011), coalescent stochasticity (Carstens et al. 2005), the misinterpretation of coalescent time in common ancestors as part of species divergence by BEAST (Angelis and dos Reis 2015), or misspecification of the substitution rate.

Our results suggest a relatively old divergence between *S. magister* and *S. zosteromus* with little-to-no evidence of introgression between them, including in the northern region of the peninsula where their ranges come together. Grismer and McGuire (1996) also failed to find morphological evidence of hybridization in the area despite sympatry. On the other hand,

our sNMF results indicate admixture in the southern Baja California Peninsula. Dispersal over the Gulf of California has been proposed before for several taxa (Grismer 1994; Murphy and Aguirre-León 2002; Wood et al. 2008; Garrick et al. 2009). It has been suggested that trans-gulf dispersal occurred across a chain of islands between southern Baja California and central Sonora, likely when sea levels were low (Grismer 1994; Carreño and Helenes 2002; Wood et al. 2008). Obtaining genomic data for *S. lineatulus* would be important to test this hypothesis, as that insular taxon is geographically intermediate between *S. magister* and admixed individuals of *S. zosteromus* (Figs. 1b and 3). However, most of our present results suggest that the limited amount of shared ancestry between *S. magister* and *S. zosteromus* (Fig. 3) is likely due to incomplete lineage sorting (ILS). The IM results from BPP suggest that migration between SB and SD is insignificant. Populations in the *S. magister* complex are either arboreal, terrestrial, or saxicolous (Parker and Pianka 1973; Parker 1982). Thus, constant migration by swimming seems extremely unlikely, and rafting may not occur at a frequency high enough to leave a genetic signal.

### Phylogeography of *S. magister*

All splits in *S. magister* are estimated to have occurred during the Pleistocene, presumably supporting a glacial refugia model of divergence. Significant gene flow between SD and MD indicates that there was likely secondary contact following allopatric divergence. However, our analyses cannot refute the hypothesis of divergence with gene flow between these populations. The order of divergences within the species is equivocal. The topology obtained using the GBS data disagrees with that of the mtDNA. In the GBS tree, the SD and MD populations are reciprocally monophyletic, whereas this is not true in the mtDNA topology. Instead, the individuals allied to SD are mixed within a clade of MD samples. In other words, many lizards with an MD nuclear background possess SD-like mtDNA. Although these patterns could be explained by ILS, our IM analyses recovered nuclear gene flow between these populations that could have been accompanied by mtDNA introgression. We note that concatenation and single-locus approaches are vulnerable to high levels of ILS, especially when fast speciation and large effective population sizes promote the appearance of strongly supported gene trees that do not match the species tree

(Linkem et al. 2016; Mendes and Hahn 2018). Our species tree analyses support an early divergence of populations in the Chihuahuan Desert—a common though not universal pattern in co-distributed taxa (Mulcahy 2008; Myers et al. 2017; O'Connell et al. 2017; Chafin et al. 2021; Santibáñez-López et al. 2021).

Our results suggest that both the WCD and Colorado River are acting as barriers to gene flow in *S. magister*. Population structure, phylogenetic analyses, and the evaluation of isolation all suggest that there is some degree of differentiation between the populations occurring on each side of these features. Effective migration is lower than expected across both landmarks and the GDMs identify barriers as the strongest predictors of genetic distance. However, there are notable differences in the nature and strength of the 2 barriers.

The WCD appears to be a remarkably strong barrier. All individuals east of it belong to the CD clade in both the nuclear and mitochondrial trees, most of those individuals have a tiny fraction of ancestry from other populations, and CD appears to be highly isolated (based on multiple lines of evidence). Ecological Niche Model (ENM) tests of identity and linear range break also corroborated the relevance of the WCD as a relevant climatic barrier (Table 2), where lineages on both sides have likely differentiated ecological niches. Additionally, EEMS identifies areas of low effective migration that overlap with portions of the WCD (Fig. 6). Furthermore, the barrier explains over 75% of the deviance in genetic distance, much more than that explained by climatic and geographic distances (Supplementary Table S7). Where the Chihuahuan and Sonoran Deserts meet, the WCD is represented by the Cochise Filter Barrier, an ecotonal region of arid grasslands and scrublands (Castoe et al. 2007; Laport et al. 2012; Myers et al. 2019b). Climatic suitability for *S. magister* is apparently low in the area, particularly during glacial periods. Fragmentation of arid habitat in the area may have started during the Pliocene (Morafka 1977), and the region may have been vegetated by mesic woodlands as recently as 4 kya (Van Devender 1990), thus driving divergence between arid-adapted lineages (Castoe et al. 2007). Recent studies suggest that the strength of this barrier and the timing of divergences associated with it are not uniform across taxa (Myers et al. 2017, 2019b), and may be related to differences in vagility and thermal ecology (Provost et al. 2021). This could explain the divergence across the Cochise Filter Barrier in *S. magister*. Individuals of *S. magister* are territorial and have small home ranges (Tanner and Krogh 1973). Furthermore, climate change may have a stronger influence on the ranges of ectotherms, and they may be more prone to local adaptation which can promote divergence (Keller and Seehausen 2012; Wogan and Richmond 2015; Provost et al. 2021).

There is an isolated individual from southern Chihuahua in the CD population that possessed substantial ancestry from MD (Fig. 3a) and is placed sister to the remaining CD individuals in all phylogenetic

analyses (Fig. 4; Supplementary Figs. S4–S6). This result could be taken as evidence that the WCD is weaker as a barrier in Mexico, allowing occasional gene flow with other *S. magister* populations. However, the WCD actually reaches its highest altitude in the Sierra Madre Occidental of Mexico, an old (Oligocene–Miocene) mountain range covered by mesic forest (Bye 1995; Ferrari et al. 2005). In addition, our IM models in BPP provided weak evidence of gene flow between CD and MD (Supplementary Table S3). Instead, the mixed ancestry of the Chihuahuan individual could point to retained ancestral polymorphism (ILS). It can be difficult to distinguish between gene flow and ancestral polymorphism (Muir and Schlötterer 2005; Lexer et al. 2006). The Chihuahuan lizard comes from the Bolsón de Mapimí, an endorheic basin that has been previously identified as a refugium and area of high genetic diversity (Myers et al. 2019a; Scheinvar et al. 2020). Accordingly, the region was identified as an area of high environmental suitability for *S. magister* relative to surrounding regions during the LGM (Supplementary Fig. S7). The high stability of refugia has been associated with high genetic diversity (Carnaval et al. 2009). Additional sampling in Mexico seems necessary to test for differences in the genetic diversity of *S. magister* across the Chihuahuan Desert.

Our results suggest that the Colorado River is acting as a barrier to gene flow. The distributions of SD and MD appear to be bounded by this feature. Effective migration is lower than expected in the lower reaches of the river (Fig. 6a). Furthermore, the GDM analyses suggest that the river explains more variation in genetic distances than climatic or geographic distances (but see below). Additionally, none of our potential distribution predictions detect discontinuity in suitable habitat along the river, showing that it must be the feature itself and not climate that is driving isolation (Supplementary Fig. S7). This was corroborated by linear range break tests indicating no statistically significant steep climatic transitions at both sides of the Colorado River, evidencing that the region is acting as a physical barrier, rather than a climatic one (Table 2). However, several analyses support the Colorado River as a porous barrier. The connection of the Colorado River and the Gulf of California is thought to have occurred between the Late Miocene and Early Pliocene (Dolby et al. 2019; Nicholson et al. 2019), but the split between SD and MD occurred in the Pleistocene. Thus, our results refute the hypothesis that the original formation of the Colorado River and/or marine incursions from the Gulf of California caused vicariance. Furthermore, the estimation of ancestry coefficients and migration rates indicate that there is bidirectional migration across the river. The migration rate from MD to SD is higher than from SD to MD (Fig. 5) and individuals with high ancestry from MD are found east of the river (Fig. 3a), consistent with a previous meta-analysis suggesting that west–east migration may be more common than vice versa (Dolby et al. 2019). It is possible that gene flow occurred during the

MIS-9 interglacial period—perhaps one of the warmest Pleistocene interglacials (Yin and Berger 2015)—when the expansion of suitable habitat for *S. magister* may have enabled secondary contact. The mtDNA data are also consistent with introgression between MD and SD. On the other hand, the GDM indicates that climate has a joint predictive power that is almost as high as that of the river (Fig. 7). Finally, the GDI indicates poor differentiation between the populations occurring west of the WCD. Our study agrees with cumulative evidence suggesting that the Colorado River is best characterized as a permeable barrier (Smith et al. 2011; Dolby et al. 2019). In *S. magister*, genetic structure west of the WCD is best explained by the combined effects of the Colorado River, climatic variation, and geographic distance to a lesser extent. Isolation driven by adaptation to local climate may be a determinant factor for divergence in the region (Dolby et al. 2019; Myers et al. 2019b) and, as explained above, may have a larger effect on ectotherms.

The Colorado River appears to be playing a dual role in the geographic structuring of *S. magister*. The Lower Colorado River acts as a soft barrier to gene flow, whereas northern regions may be enabling connectivity among the MD lineage. Our distribution models show that narrow strips of suitable habitat along the river connect the ranges of MD populations, where the Little Colorado and San Juan rivers connect with the Colorado River (Supplementary Fig. S7). EEMS also suggests that effective migration is high along portions of this corridor (Fig. 6a). The eastern Gila River, which lies northeast of the Sonoran Desert, also appears to be acting as a corridor that has allowed the propagation of MD into the range of SD. Individuals with mixed ancestry from MD and SD are found along the San Simon Valley, the intermittent wash of which leads to the eastern Gila River in this region (Figs. 1a and 3a). Populations in this area (and one specimen from Tucson) were historically assigned to the subspecies *S. m. bimaculosus* (Fig. 1). However, the GBS and mtDNA data both agree that the WCD represents the major barrier between the SD and CD populations, and the geographic distribution of the MD and SD lineages also appear loosely demarcated along the Gila River. The relative roles of the Colorado versus Gila Rivers in structuring genetic and species diversity should be explored in subsequent studies with more sampling in this region.

#### Phylogeography of *S. zosteromus*

The distribution of the 2 highly differentiated clades in *S. zosteromus* could be misinterpreted as support for the Mid-Peninsular Seaway hypothesis. However, when carefully considered, the causes of geographic structure in the species are ambiguous. EEMS suggests that IBD roughly predicts genetic dissimilarity around the barrier, and ENM results suggest that there are neither differences in the climatic niche between both lineages nor steep environmental gradients on either side of the barrier (Table 2). Overall, this suggests that the

division between the lineages may be caused by a geographic rather than a climatic barrier. However, the mid-peninsular region is bordered by the Vizcaíno Desert to the north, an area that has low climatic suitability for *S. zosteromus*, particularly during the present and LIG climatic conditions (Supplementary Fig. S7). Conversely, the GDM analyses revealed that climate is the best independent predictor of genetic distance, hinting at an IBE pattern of gradual genetic differentiation along an environmental gradient. The “barrier” had the largest joint effect on genetic distance in the GDM results when PCA was applied to the climatic variables. Finally, the basal split in *S. zosteromus* is estimated to have occurred during the Pliocene-Pleistocene transition, which is younger than geologically supported marine incursions in the Peninsula (Late Miocene–Early Pliocene) (Lindell et al. 2006), and instead could be associated with increased aridification (Axelrod 1979). We consider that these discrepancies are likely driven by sampling. The analyses based on the molecular data are evidently limited by small sample sizes. The analyses based on ENM may seem more robust given the larger sample sizes due to the incorporation of collection records. However, our division of these records into northern and southern groups was based on the position of the seaway proposed in previous studies. More accurate characterization of niche divergence between the lineages would instead require pinpointing the geographic location of the genetic break between northern and southern *S. zosteromus*, which we could not do given our sampling.

The high predictive power of the Mid-Peninsular Seaway in phylogeographic studies could likely be the result of its post hoc geographic placement. The seaway is not related to an obvious feature such as the Colorado River or WCD. Instead, the position of the “barrier” is largely based on the observed location of genetic splits in several taxa (Riddle et al. 2000; Lindell and Murphy 2008; Dolby et al. 2015). Alternative explanations for these genetic breaks, such as sharp climatic transitions or past climate change, remain untested in studies that rely solely on molecular data. Fine-scale sampling, comparative multi-taxon approaches, and integrative analyses of environmental, geological, and biological data may be necessary to tease apart the drivers of divergence across the Baja California Peninsula (Riddle et al. 2000; Dolby et al. 2015, 2022; Cab-Sulub and Álvarez-Castañeda 2021).

#### Mechanisms of Divergence in the *S. magister* Complex

Our results hint at some of the biological mechanisms responsible for the divergence of geographic lineages in the *S. magister* complex. As shown above, the age of the split between *S. magister* and *S. zosteromus* is contemporary with the formation of the Gulf of California, suggesting vicariance. Although more detailed analyses of demographic history are necessary, the allelic diversity of the Chihuahuan individual together with the phylogenetic placement of CD suggest that *S. magister* could have originated in the southeastern portion of

its current range. Alternatively, *S. magister* may have originated in the SD region and expanded north and east. The relatively small CD population may have originated by a founder event, which was subsequently cut off by the WCD. This hypothesis is supported by both relative population size estimates and spatial patterns of genomic diversity. The diverse allelic makeup of southern *S. zosteromus* (Fig. 3a) could also indicate a southern origin (Austerlitz et al. 1997; Peter and Slatkin 2013), which is also supported by our EEMS and BPP analyses. Thus, the sympatry of *S. magister* and *S. zosteromus* in northern Baja California likely followed the expansion of both species' ranges, forming a ring distribution around the Gulf of California similar to *Hypsilegra* nightsnakes (Mulcahy and Macey 2009). Furthermore, an initial southern split agrees with the older rifting of the southern Peninsula of Baja California, as has been supported by geological (Ferrari 1995) and biological evidence (Mulcahy and Macey 2009). Our results and morphological data (Grismer and McGuire 1996) suggest that these species are reproductively isolated in northern Baja California. Local adaptation (as suggested by the ENMs) and other evolutionary forces could have already produced reproductive isolation before secondary contact. However, it is also possible that speciation reinforcement occurred in northern Baja California in the past, providing an alternative explanation for the greater genetic differentiation between the species in the northwestern portions of their range (Fig. 3a).

Vicariance also seems to be responsible for the divergence between CD and other *S. magister*, with the WCD acting as a strong barrier to gene flow. We found no evidence for continuous gene flow or secondary contact between lineages on both sides of the Divide other than the admixed Chihuahuan individual and the nested position of CD in the mitochondrial genealogy, both of which could have alternative explanations (see above). Conversely, our results point to more complex scenarios for the divergence between MD and SD on one hand and NB and SB on the other. Unfortunately, our sampling is poor for the latter pair. Regarding MD and SD, it is clear that the Colorado River is responsible for some degree of differentiation (see above). However, allopatric divergence alone offers a poor explanation for genetic differentiation. Environmental gradients are also an accurate predictor of genetic structure (Fig. 7), meaning that IBE is acting in synergy with the barrier posed by the Colorado River to promote divergence. Both theoretical models and empirical evidence show that environmental gradients can promote evolutionary divergence despite resistance from gene flow (Doebeli and Dieckmann 2003; Myers et al. 2019b). Scanning for signs of local adaptation in the genome and modeling the genomic signature of complex, multi-factorial scenarios could shed light on how barriers and gradients interact to generate and sort genetic variation. On the other hand, it is unclear whether the parapatry and mixed ancestry in the contact zone of these two lineages is the result of secondary contact following range

expansion or divergence with gene flow. The modeling and comparison of alternative demographic scenarios is necessary to positively distinguish between these 2 alternatives.

## CONCLUSIONS AND TAXONOMIC IMPLICATIONS

Patterns of gene flow and isolation in Desert Spiny Lizards are tightly linked to the history of their desert habitat in western North America. While recent studies have questioned the importance of biogeographic barriers as drivers of isolation in the region, our results suggest that barriers have played a central role in the geographic sorting of genetic diversity in these lizards. This suggests that the impact of barriers may be taxon-specific and related to biological features such as dispersal ability and ecological requirements. Our study also emphasizes how a thorough analysis of molecular and environmental data is needed to avoid mischaracterizing the nature and strength of purported barriers to gene flow. In addition, our results suggest that gene flow and local adaptation are acting simultaneously on the group. The dynamics of local adaptation with gene flow are complex, and Desert Spiny Lizards may be an adequate system to address these issues. Large-scale comparative and integrative studies of Nearctic taxa are needed to resolve some unsettled questions. What ecological traits are correlated with higher degrees of differentiation? What factors are promoting divergence in the Baja California Peninsula? Is the evolutionary history of arid-adapted taxa characterized by isolation with gene flow or by secondary contact following allopatric divergence? Furthermore, whole genome sequencing could shed light on how adaptation to local environmental conditions is driving divergence in the region.

Finally, our analyses provide compelling evidence that some populations in the *S. magister* complex may be reproductively isolated and warrant taxonomic revision. Our results support the conspecificity of the *S. magister* populations that are morphologically assignable to *S. m. magister*, *S. m. cephaloflavus*, *S. m. transversus*, and *S. m. uniformis*. On the other hand, clustering, phylogenetic analysis of GBS and mtDNA data, and gene flow analyses suggest that CD is reproductively isolated. In contrast with morphological taxonomy (Fig. 1b), our results indicate that this lineage is restricted to the Chihuahuan Desert east of the WCD (Figs. 3 and 4). Previous studies have recommended that this population be formally recognized as *S. bimaculosus* (Schulte II et al. 2006). However, until additional data are collected (e.g., morphology) and sampling in Mexico is improved, we refrain from recognizing *S. bimaculosus*. For the time being, we consider *S. magister* as monotypic as suggested by Leaché and Mulcahy (2007). In the Peninsula of Baja California, evidence suggests that *S. z. zosteromus* and *S. z. monserratensis* are not evolutionarily independent. In contrast, *S. z. rufidorsum* appears to be divergent. However, given our limited sample sizes and

previously published patterns of morphological and molecular variation (Grismar and McGuire 1996), we treat *S. zosteromus* as monotypic. Until further sampling is possible, we recognize *S. lineatulus* given its morphological distinctness (Grismar and McGuire 1996). Ultimately, comprehensive sampling and morphological data may provide additional insight into species limits and the ecological and evolutionary processes underlying reproductive isolation in the complex.

#### SUPPLEMENTARY MATERIAL

Data available from the Dryad Digital Repository: [https://datadryad.org/stash/share/1Mtqy-Id6SFsTSm26KFTEERhihF4X1fnpC56E71\\_khE](https://datadryad.org/stash/share/1Mtqy-Id6SFsTSm26KFTEERhihF4X1fnpC56E71_khE).

#### ACKNOWLEDGMENTS

We thank R.C. Clark (Dancing Snake Nature Photography) and A.G. Clause for allowing us to use their photographs in Figs. 1 and 4, respectively. We also thank E.A. Pavón Vázquez for assistance with bioinformatics and I. Overcast for his assistance with ipyrad. Finally, we thank the following individuals and institutions for providing tissue samples: G. Watkins-Colwell (Yale Peabody Museum), L. Scheinberg (California Academy of Sciences), C. Spencer (Museum of Vertebrate Zoology), A. Lathrop and R. Murphy (Royal Ontario Museum), and S. Birks and P. Miller (Burke Museum Genetic Resources Collection). This study was, in part, facilitated by institutional computational resources. The CUNY HPCC is operated by the College of Staten Island. The NMNH-LAB (Smithsonian Institution) provided computer support for D.G.M.

#### FUNDING

This work was supported by grants from the National Science Foundation (NSF) to C.B. (DEB-1929679) and A.D.L. (DEB-2023723); Biotechnology and Biological Sciences Research Council (BB/T003502/1, BB/X007553/1) and Natural Environment Research Council grants (NE/X002071/1) to Z.Y.; and an NSF Graduate Research Fellowship to K.F. (Award #2037786). The CUNY HPCC is partially funded by grants from the City of New York, State of New York, CUNY Research Foundation, and NSF grants CNS-0958379, CNS-0855217, and ACI 1126113.

#### DATA AVAILABILITY

Data available from the Dryad Digital Repository: [https://datadryad.org/stash/share/1Mtqy-Id6SFsTSm26KFTEERhihF4X1fnpC56E71\\_khE](https://datadryad.org/stash/share/1Mtqy-Id6SFsTSm26KFTEERhihF4X1fnpC56E71_khE)

#### REFERENCES

Angelis K., dos Reis M. 2015. The impact of ancestral population size and incomplete lineage sorting on Bayesian estimation of species divergence times. *Curr. Zool.* 61:874–885.

Austerlitz F., Jung-Muller B., Godelle B., Gouyon P.-H. 1997. Evolution of coalescence times, genetic diversity and structure during colonization. *Theor. Popul. Biol.* 51:148–164.

Avise J.C. 2000. *Phylogeography: the history and formation of species*. Cambridge: Harvard University Press.

Axelrod D.I. 1979. Age and origin of Sonoran desert vegetation. *Occas. Pap. Calif. Acad. Sci.* 132:1–74.

Bell E.L., Smith H.M., Chiszar D. 2003. An annotated list of the species-group names applied to the lizard genus *Sceloporus*. *Act. Zool. Mex.* 90:103–174.

Brown J.L., Hill D.J., Dolan A.M., Carnaval A.C., Haywood A.M. 2018. PaleoClim, high spatial resolution paleoclimate surfaces for global land areas. *Sci. Data*. 5:1–9.

Bryson R.W.Jr., García-Vázquez U.O., Riddle B.R. 2012. Diversification in the Mexican horned lizard *Phrynosoma orbiculare* across a dynamic landscape. *Mol. Phylogenetic Evol.* 62:87–96.

Bye R. 1995. Prominence of the Sierra Madre Occidental in the biological diversity of Mexico. In: USDA Forest Service Rocky Mountain Forest and Range Experiment Station, editor. *Biodiversity and management of the Madrean Archipelago: the sky islands of the Southwestern United States and Northwestern Mexico*. Fort Collins: USDA Forest Service Rocky Mountain Forest and Range Experiment Station. p. 19–27.

Cab-Sulub L., Álvarez-Castañeda S.T. 2021. Climatic dissimilarity associated with phylogenetic breaks. *J. Mammal.* 102:1592–1604.

Carnaval A.C., Hickerson M.J., Haddad C.F.B., Rodrigues M.T., Moritz C. 2009. Stability predicts genetic diversity in the Brazilian Atlantic Forest hotspot. *Science* 323:785–789.

Carreño A.L., Helenes J. 2002. Geology and ages of the islands. In: Case T.J., Cody M.L., Ezcurra E., editors. *A new island biogeography of the Sea of Cortés*. New York (NY): Oxford University Press. p. 14–40.

Carstens B.C., Degenhardt J.D., Stevenson A.L., Sullivan J. 2005. Accounting for coalescent stochasticity in testing phylogeographical hypotheses: modelling Pleistocene population structure in the Idaho giant salamander *Dicamptodon aterrimus*. *Mol. Ecol.* 14:255–265.

Castoe T.A., Spencer C.L., Parkinson C.L. 2007. Phylogeographic structure and historical demography of the western diamondback rattlesnake (*Crotalus atrox*): a perspective on North American desert biogeography. *Mol. Phylogenetic Evol.* 42:193–212.

Chafin T.K., Douglas M.R., Anthony Samy W.J.B., Sullivan B.K., Walker J.M., Cordes J.E., Douglas M.E. 2021. Taxonomic hypotheses and the biogeography of speciation in the Tiger Whiptail complex (*Aspidoscelis tigris*: Squamata, Teiidae). *Front. Biogeogr.* 13:49120.

Chifman J., Kubatko L. 2014. Quartet inference from SNP data under the coalescent model. *Bioinformatics* 30:3317–3324.

Cobos M.E., Peterson A.T., Barve N., Osorio-Olvera L. 2019. kuenm: an R package for detailed development of ecological niche models using Maxent. *PeerJ* 7:e6281.

Doebeli M., Dieckmann U. 2003. Speciation along environmental gradients. *Nature* 421:259–264.

Dolby G.A., Bennett S.E.K., Dorsey R.J., Stokes M.F., Riddle B.R., Lira-Noriega A., Munguia-Vega A., Wilder B.T. 2022. Integrating Earth-life systems: a geogenomic approach. *Trends Ecol. Evol.* 37:371–384.

Dolby G.A., Bennett S.E.K., Lira-Noriega A., Wilder B.T., Munguía-Vega A. 2015. Assessing the geological and climatic forcing of biodiversity and evolution surrounding the Gulf of California. *J. Southwest.* 57:391–455.

Dolby G.A., Dorsey R.J., Graham M.R. 2019. A legacy of geo-climatic complexity and genetic divergence along the lower Colorado River: insights from the geological record and 33 desert-adapted animals. *J. Biogeogr.* 46:2479–2505.

dos Reis M. 2022. bppr: an R package for BPP. R package version 0.6.1. Available from: <https://drrii.github/dosreislab/bppr/>.

Eaton D.A.R., Overcast I. 2020. ipyrad: Interactive assembly and analysis of RADseq datasets. *Bioinformatics* 36:2592–2594.

Environmental Protection Agency. 2018. Ecoregions of North America. Environmental Protection Agency. Available from: <https://data.usda.gov/dataset/ecoregions-north-america>.

Farleigh K., Vladimirova S.A., Blair C., Bracken J.T., Koochekian N., Schield D.R., Card D.C., Finger N., Henault J., Leaché A.D., Castoe T.A., Jezkova T. 2021. The effects of climate and demographic history in shaping genomic variation across populations of the Desert Horned Lizard (*Phrynosoma platyrhinos*). *Mol. Ecol.* 30:4481–4496.

Fehlberg S.D., Ranker T.A. 2009. Evolutionary history and phyogeography of *Encelia farinosa* (Asteraceae) from the Sonoran, Mojave, and Peninsular Deserts. *Mol. Phylogenet. Evol.* 50:326–335.

Fenker J., Tedeschi L.G., Melville J., Moritz C. 2021. Predictors of phylogeographic structure among codistributed taxa across the complex Australian monsoonal tropics. *Mol. Ecol.* 30:4276–4291.

Ferrari L. 1995. Miocene shearing along the northern boundary of the Jalisco block and the opening of the southern Gulf of California. *Geology*. 23:751–754.

Ferrari L., Valencia-Moreno M., Bryan S., Ferrari L., Valencia-Moreno M., Bryan S. 2005. Magmatism and tectonics of the Sierra Madre Occidental and its relation with the evolution of western North America. *Bol. Soc. Geol. Mex.* 57:343–378.

Frerier S., Manion G., Elith J., Richardson K. 2007. Using generalized dissimilarity modelling to analyse and predict patterns of beta diversity in regional biodiversity assessment. *Divers. Distrib.* 13:252–264.

Fick S.E., Hijmans R.J. 2017. WorldClim 2: new 1-km spatial resolution climate surfaces for global land areas. *Int. J. Climatol.* 37:4302–4315.

Finger N., Farleigh K., Bracken J.T., Leaché A.D., François O., Yang Z., Flouri T., Charran T., Jezkova T., Williams D.A., Blair C. 2022. Genome-scale data reveal deep lineage divergence and a complex demographic history of the Texas horned lizard (*Phrynosoma cornutum*) throughout the southwestern and central United States. *Genome Biol. Evol.* 14:evab260.

Fitzpatrick M., Mokany K., Manion G., Nieto-Lugilde D., Ferrier S. 2021. gdm: generalized dissimilarity modeling. R package version 1.5.0-1. Available from: <https://CRAN.R-project.org/package=gdm>.

Flouri T., Jiao X., Rannala B., Yang Z. 2018. Species tree inference with BPP using genomic sequences and the multispecies coalescent. *Mol. Biol. Evol.* 35:2585–2593.

Flouri T., Jiao X., Rannala B., Yang Z. 2020. A Bayesian implementation of the multispecies coalescent model with introgression for phylogenomic analysis. *Mol. Biol. Evol.* 37:1211–1223.

Frichot E., François O. 2015. LEA: An R package for Landscape and Ecological Association studies. *Methods Ecol. Evol.* 6:925–929.

Frichot E., Mathieu F., Trouillon T., Bouchard G., François O. 2014. Fast and efficient estimation of individual ancestry coefficients. *Genetics* 196:973–983.

Garrick R.C., Nason J.D., Meadows C.A., Dyer R.J. 2009. Not just vicariance: phylogeography of a Sonoran Desert euphorb indicates a major role of range expansion along the Baja peninsula. *Mol. Ecol.* 18:1916–1931.

Glor R.E., Warren D. 2011. Testing ecological explanations for biogeographic boundaries. *Evolution*. 65:673–683.

Grismer L.L. 1994. Geographic origins for the reptiles on islands in the Gulf of California, Mexico. *Herpetol. Nat. Hist.* 2:17–41.

Grismer L.L. 2002. A re-evaluation of the evidence for a Mid-Pleistocene mid-peninsular seaway in Baja California: a reply to Riddle et al. *Herpetol. Rev.* 33:15–16.

Grismer L.L., McGuire J.A. 1996. Taxonomy and biogeography of the *Sceloporus magister* complex (Squamata: Phrynosomatidae) in Baja California, México. *Herpetologica*. 52:416–427.

Gronau I., Hubisz M.J., Gulk B., Danko C.G., Siepel A. 2011. Bayesian inference of ancient human demography from individual genome sequences. *Nat. Genet.* 43:1031–1034.

Guindon S., Dufayard J.F., Lefort V., Anisimova M., Hordijk W., Gascuel O. 2010. New algorithms and methods to estimate maximum-likelihood phylogenies: assessing the performance of PhyML 3.0. *Syst. Biol.* 59:307–321.

Hey J., Chung Y., Sethuraman A., Lachance J., Tishkoff S., Sousa V.C., Wang Y. 2018. Phylogeny estimation by integration over isolation with migration models. *Mol. Biol. Evol.* 35:2805–2818.

Hijmans R.J., Phillips S., Leathwick J., Elith J. 2022. dismo: species distribution modeling. R package version 1.3-9. Available from: <https://CRAN.R-project.org/package=dismo>.

Hoang D.T., Chernomor O., von Haeseler A., Minh B.Q., Vinh L.S. 2018. UFBoot2: improving the ultrafast bootstrap approximation. *Mol. Biol. Evol.* 35:518–522.

Jackson N.D., Carstens B.C., Morales A.E., O'Meara B.C. 2017. Species delimitation with gene flow. *Syst. Biol.* 66:799–812.

Jaynes K.E., Myers E.A., Gvoždík V., Blackburn D.C., Portik D.M., Greenbaum E., Jongsma G.F.M., Rödel M.O., Badjedjea G., Bamba-Kaya A., Baptista N.L., Akuboy J.B., Ernst R., Kouete M.T., Kusamba C., Masudi F.M., McLaughlin P.J., Nneji L.M., Onadeko A.B., Penner J., Vaz Pinto P., Stuart B.L., Tobi E., Zassi-Boulou A.G., Leaché A.D., Fujita M.K., Bell R.C. 2022. Giant Tree Frog diversification in West and Central Africa: isolation by physical barriers, climate, and reproductive traits. *Mol. Ecol.* 31:3979–3998.

Ji J., Jackson D.J., Leaché A.D., Yang Z. 2023. Power of Bayesian and heuristic tests to detect cross-species introgression with reference to gene flow in the *Tamias quadrivittatus* group of North American chipmunks. *Syst. Biol.* 72:sysac077.

Jordan D.S. 1905. The origin of species through isolation. *Science* 22:545–562.

Karger D.N., Nobis M.P., Normand S., Graham C.H., Zimmermann N.E. 2023. CHELSA-TraCE21k—high-resolution (1°) downscaled transient temperature and precipitation data since the Last Glacial Maximum. *Clim. Past* 19:439–456.

Keller I., Seehausen O. 2012. Thermal adaptation and ecological speciation. *Mol. Ecol.* 21:782–799.

Kornai D., Flouri T., Yang Z. 2023. Hierarchical heuristic species delimitation under the multispecies coalescent model with migration. *bioRxiv* 2023.09.10.557025.

Lamb T., Jones T.R., Avise J.C. 1992. Phylogeographic histories of representative herpetofauna of the southwestern U.S.: mitochondrial DNA variation in the desert iguana (*Dipsosaurus dorsalis*) and the chuckwalla (*Sauromalus obesus*). *J. Evol. Biol.* 5:465–480.

Laport R.G., Minckley R.L., Ramsey J. 2012. Phylogeny and cytogeography of the North American Creosote Bush (*Larrea tridentata*, Zygophyllaceae). *Syst. Bot.* 37:153–164.

Leaché A.D., Banbury B.L., Felsenstein J., Nieto-Montes de Oca A., Stamatakis A. 2015a. Short tree, long tree, right tree, wrong tree: new acquisition bias corrections for inferring SNP phylogenies. *Syst. Biol.* 64:1032–1047.

Leaché A.D., Banbury B.L., Linkem C.W., Nieto-Montes de Oca A. 2016. Phylogenomics of a rapid radiation: is chromosomal evolution linked to increased diversification in north american spiny lizards (Genus *Sceloporus*)? *BMC Evol. Biol.* 16:63–16.

Leaché A.D., Chavez A.S., Jones L.N., Grummer J.A., Gottscho A.D., Linkem C.W. 2015b. Phylogenomics of phrynosomatid lizards: conflicting signals from sequence capture versus restriction site associated DNA sequencing. *Genome Biol. Evol.* 7:706–719.

Leaché A.D., Crews S.C., Hickerson M.J. 2007. Two waves of diversification in mammals and reptiles of Baja California revealed by hierarchical Bayesian analysis. *Biol. Lett.* 3:646–650.

Leaché A.D., Mulcahy D.G. 2007. Phylogeny, divergence times and species limits of spiny lizards (*Sceloporus magister* species group) in western North American deserts and Baja California. *Mol. Ecol.* 16:5216–5233.

Leaché A.D., Zhu T., Rannala B., Yang Z. 2019. The spectre of too many species. *Syst. Biol.* 68:168–181.

Lee J., Miller M.M., Crippen R., Hacker B., Ledesma Vazquez J. 1996. Middle Miocene extension in the Gulf Extensional Province, Baja California: evidence from the southern Sierra Juarez. *GSA Bull.* 108:505–525.

Lexer C., Kremer A., Petit R.J. 2006. Shared alleles in sympatric oaks: recurrent gene flow is a more parsimonious explanation than ancestral polymorphism. *Mol. Ecol.* 15:2007–2012.

Lindell J., Murphy R.W. 2008. Simple identification of mitochondrial lineages in contact zones based on lineage-selective primers. *Mol. Ecol. Resour.* 8:66–73.

Lindell J., Ngo A., Murphy R.W. 2006. Deep genealogies and the mid-peninsular seaway of Baja California. *J. Biogeogr.* 33:1327–1331.

Linkem C.W., Minin V.N., Leaché A.D. 2016. Detecting the anomaly zone in species trees and evidence for a misleading signal in higher-level skink phylogeny (Squamata: Scincidae). *Syst. Biol.* 65:465–477.

Loera I., Sosa V., Ickert-Bond S.M. 2012. Diversification in North American arid lands: niche conservatism, divergence and expansion of habitat explain speciation in the genus *Ephedra*. *Mol. Phylogenet. Evol.* 65:437–450.

Macey J.R., Wang Y., Ananjeva N.B., Larson A., Papenfuss T.J. 1999. Vicariant patterns of fragmentation among gekkonid lizards of the genus *Teratoscincus* produced by the Indian collision: a molecular phylogenetic perspective and an area cladogram for central Asia. *Mol. Phylogenet. Evol.* 12:320–332.

Manthey J.D., Moyle R.G. 2015. Isolation by environment in White-breasted Nuthatches (*Sitta carolinensis*) of the Madrean Archipelago sky islands: a landscape genomics approach. *Mol. Ecol.* 24:3628–3638.

Mayr E. 1963. Animal species and evolution. Cambridge: Harvard University Press.

Mendes F.K., Hahn M.W. 2018. Why concatenation fails near the anomaly zone. *Syst. Biol.* 67:158–169.

Minh B.Q., Schmidt H.A., Chernomor O., Schrempf D., Woodhams M.D., von Haeseler A., Lanfear R. 2020. IQ-TREE 2: new models and efficient methods for phylogenetic inference in the genomic era. *Mol. Biol. Evol.* 37:1530–1534.

Mokany K., Ware C., Woolley S.N.C., Ferrier S., Fitzpatrick M.C. 2022. A working guide to harnessing generalized dissimilarity modeling for biodiversity analysis and conservation assessment. *Global Ecol. Biogeogr.* 31:802–821.

Morafka D.J. 1977. A biogeographical analysis of the Chihuahuan Desert through its herpetofauna. The Hague: Dr. W. Junk bv, Publishers.

Muir G., Schlötterer C. 2005. Evidence for shared ancestral polymorphism rather than recurrent gene flow at microsatellite loci differentiating two hybridizing oaks (*Quercus* spp). *Mol. Ecol.* 14:549–561.

Mulcahy D.G. 2008. Phylogeography and species boundaries of the western North American Nightsnake (*Hypsiglena torquata*): revisiting the subspecies concept. *Mol. Phylogenet. Evol.* 46:1095–1115.

Mulcahy D.G., Macey J.R. 2009. Vicariance and dispersal form a ring distribution in nightsnakes around the Gulf of California. *Mol. Phylogenet. Evol.* 53:537–546.

Murphy RW., Aguirre-León G. 2002. The nonavian reptiles: origins and evolution. In: Case T.J., Cody M.L., Ezcurra E., editors. A new island biogeography of the Sea of Cortés. New York: Oxford University Press. p. 181–220.

Myers E.A., Bryson R.W.Jr., Hansen R.W., Aardema M.L., Lazcano D., Burbrink F.T. 2019a. Exploring Chihuahuan Desert diversification in the gray-banded kingsnake, *Lampropeltis alterna* (Serpentes: Colubridae). *Mol. Phylogenet. Evol.* 131:211–218.

Myers E.A., Hickerson M.J., Burbrink F.T. 2017. Asynchronous diversification of snakes in the North American warm deserts. *J. Biogeogr.* 44:461–474.

Myers E.A., Xue A.T., Gehara M., Cox C.L., Davis Rabosky A.R., Lemos-Espinal J., Martínez-Gómez J.E., Burbrink F.T. 2019b. Environmental heterogeneity and not vicariant biogeographic barriers generate community-wide population structure in desert-adapted snakes. *Mol. Ecol.* 28:4535–4548.

Neiswenter S.A., Riddle B.R. 2010. Diversification of the *Perognathus flavus* species group in emerging arid grasslands of western North America. *J. Mammal.* 91:348–362.

Nicholson U., Carter A., Robinson P., Macdonald D.I.M. 2019. Eocene–Recent drainage evolution of the Colorado River and its precursor: an integrated provenance perspective from SW California. *Geol. Soc. London* 488:47–72.

O'Connell K.A., Streicher J.W., Smith E.N., Fujita M.K. 2017. Geographical features are the predominant driver of molecular diversification in widely distributed North American whipsnakes. *Mol. Ecol.* 26:5729–5751.

Orr M.R., Smith T.B. 1998. Ecology and speciation. *Trends Ecol. Evol.* 13:502–506.

Otto-Bliesner B.L., Marshall S.J., Overpeck J.T., Miller G.H., Hu A. CAPE Last Interglacial Project members. 2006. Simulating Arctic climate warmth and icefield retreat in the last interglaciation. *Science* 311: 1751–1753.

Owens H.L., Campbell L.P., Dornak L.L., Sape E.E., Barve N., Soberón J., Ingenloff K., Lira-Noriega A., Hensz C.M., Myers C.E., Peterson A.T. 2013. Constraints on interpretation of ecological niche models by limited environmental ranges on calibration areas. *Ecol. Model.* 263:10–18.

Parker W.S. 1982. *Sceloporus magister* Hallowell Desert Spiny Lizard. *Cat. Am. Amph. Rept.* 290:1–4.

Parker W.S., Pianka E.R. 1973. Notes on the ecology of the iguanid lizard, *Sceloporus magister*. *Herpetologica*. 29:143–152.

Perry B.W., Card D.C., McGlothlin J.W., Pasquesi G.I.M., Adams R.H., Schield D.R., Hales N.R., Corbin A.B., Demuth J.P., Hoffmann F.G., Vandewege M.W., Schott R.K., Bhattacharyya N., Chang B.S.W., Casewell N.R., Whiteley G., Reyes-Velasco J., Mackessy S.P., Gamble T., Storey K.B., Biggar K.K., Passow C.N., Kuo C.-H., McGaugh S.E., Bronikowski A.M., de Koning A.P.J., Edwards S.V., Pfrender M.E., Minz P., Brodie E.D., Brodie E.D., Warren W.C., Castoe T.A. 2018. Molecular adaptations for sensing and securing prey and insight into amniote genome diversity from the garter snake genome. *Genome Biol. Evol.* 10:2110–2129.

Peter B.M., Slatkin M. 2013. Detecting range expansions from genetic data. *Evolution*. 67:3274–3289.

Petkova D., Nombre J., Stephens M. 2016. Visualizing spatial population structure with estimated effective migration surfaces. *Nat. Genet.* 48:94–100.

Phelan R.L., Brattstrom B.H. 1955. Geographic variation in *Sceloporus magister*. *Herpetologica*. 11:1–14.

Phillips S.J., Anderson R.P., Schapire R.E. 2006. Maximum entropy modeling of species geographic distributions. *Ecol. Model.* 190:231–259.

Provost K.L., Myers E.A., Smith B.T. 2021. Community phylogeographic patterns reveal how a barrier filters and structures taxa in North American warm deserts. *J. Biogeogr.* 48:1267–1283.

R Core Team. 2022. R: a language and environment for statistical computing. Vienna (Austria): R Foundation for Statistical Computing. Available from: <https://www.R-project.org/>.

Rambaut A., Drummond A.J., Xie D., Baele G., Suchard M.A. 2018. Posterior summarization in Bayesian phylogenetics using Tracer 17. *Syst. Biol.* 67:901–904.

Riddle B.R., Hafner D.J., Alexander L.F., Jaeger J.R. 2000. Cryptic vicariance in the historical assembly of a Baja. *Proc. Natl. Acad. Sci. U.S.A.* 97:14438–14443.

Santibáñez-López C.E., Cushing P.E., Powell A.M., Graham M.R. 2021. Diversification and post-glacial range expansion of giant North American camel spiders in genus *Eremocosta* (Solifugae: Eremobatidae). *Sci. Rep.* 11:1–11.

Scheinvar E., Gámez N., Moreno-Letelier A., Aguirre-Planter E., Eguiarte, L. 2020. Phylogeography of the Chihuahuan Desert: diversification and evolution over the Pleistocene. In: Mandujano M.C., Pisanty I., Eguiarte L.E., editors. Plant diversity and ecology in the Chihuahuan Desert. Cham: Springer. p. 19–44.

Schulte II J.A., Macey J.R., Papenfuss T.J. 2006. A genetic perspective on the geographic association of taxa among arid North American lizards of the *Sceloporus magister* complex (Squamata: Iguanidae: Phrynosomatinae). *Mol. Phylogenet. Evol.* 39:873–880.

Sexton J.P., Hangartner S.B., Hoffmann A.A. 2014. Genetic isolation by environment or distance: which pattern of gene flow is most common? *Evolution*. 68:1–15.

Shafer A.B.A., Wolf J.B.W. 2013. Widespread evidence for incipient ecological speciation: a meta-analysis of isolation-by-ecology. *Ecol. Lett.* 16:940–950.

Shreve F. 1942. The desert vegetation of North America. *Bot. Rev.* 8:195–246.

Smith C.I., Tank S., Godsoe W., Levenick J., Strand E., Esque T., Pellmyr O. 2011. Comparative phylogeography of a coevolved community: concerted population expansions in Joshua trees and four yucca moths. *PLoS One* 6:e25628.

Soubrier J., Steel M., Lee M.S.Y., Der Sarkissian C., Guindon S., Ho S.Y.W., Cooper A. 2012. The influence of rate heterogeneity among sites on the time dependence of molecular rates. *Mol. Biol. Evol.* 29:3345–3358.

Swofford D.L. 2003. PAUP\*. Phylogenetic analysis using parsimony and other methods. Version 4. Sunderland: Sinauer Associates.

Tanner W.W., Krogh J.E. 1973. Ecology of *Sceloporus magister* at the Nevada Test Site, Nye County, Nevada. Great Basin Nat. 33:133–146.

Upton D.E., Murphy R.W. 1997. Phylogeny of the Side-Blotched Lizards (Phrynosomatidae: *Uta*) based on mtDNA sequences: support for a midpeninsular seaway in Baja California. Mol. Phylogen. Evol. 8:104–113.

Van Devender, T.R. 1990. Late Quaternary vegetation and climate of the Chihuahuan Desert, United States and Mexico. In: Bentacourt J.L., Van Devender T.R., Martin P.S., editors. Packrat middens: the last 40,000 years of biotic change. Tucson: University of Arizona Press. p. 104–133.

Wang I.J., Bradburd G.S. 2014. Isolation by environment. Mol. Ecol. 23:5649–5662.

Warren D., Glor R.E., Turelli M. 2008. Environmental niche equivalency versus conservatism: quantitative approaches to niche evolution. Evolution. 62:2868–2883.

Warren D.L., Matzke N.J., Cardillo M., Baumgartner J.B., Beaumont L.J., Turelli M., Glor R.E., Huron N.A., Simões M., Iglesias T.L., Piquet J.C., Dinnage R. 2021. ENMTools 10: an R package for comparative ecological biogeography. Ecography. 44:504–511.

Wogan G.O.U., Richmond J.Q. 2015. Niche divergence builds the case for ecological speciation in skinks of the *Plestiodon skiltonianus* species complex. Ecol. Evol. 5:4683–4695.

Wood D.A., Fisher R.N., Reeder T.W. 2008. Novel patterns of historical isolation, dispersal, and secondary contact across Baja California in the Rosy Boa (*Lichanura trivirgata*). Mol. Phylogen. Evol. 46:484–502.

Yang Z. 1995. A space-time process model for the evolution of DNA sequences. Genetics 139:993–1005.

Yin Q., Berger A. 2015. Interglacial analogues of the Holocene and its natural near future. Quat. Sci. Rev. 120:28–46.

Zheng Y., Peng R., Kuro-o M., Zeng X. 2011. Exploring patterns and extent of bias in estimating divergence time from mitochondrial DNA sequence data in a particular lineage: a case study of salamanders (order Caudata). Mol. Biol. Evol. 28:2521–2535.